Distribution Agreement

In presenting this thesis or dissertation as a partial fulfillment of the requirements for an advanced degree from Emory University, I hereby grant to Emory University and its agents the non-exclusive license to archive, make accessible, and display my thesis or dissertation in whole or in part in all forms of media, now or hereafter known, including display on the world wide web. I understand that I may select some access restrictions as part of the online submission of this thesis or dissertation. I retain all ownership rights to the copyright of the thesis or dissertation. I also retain the right to use in future works (such as articles or books) all or part of this thesis or dissertation.

Signature:

_____ _____

Dan L. Pong Date

Translational Regulation of Kv4.2 in a Fragile X Mouse Model

By

Dan L. Pong
Master of Science
Biology

_____
Gary J. Bassell, Ph.D.
Advisor

_____
Ping Chen, Ph.D.
Committee Member

_____
Arthur English, Ph.D.
Committee Member

_____
Patricia Marsteller, Ph.D.
Committee Member

_____
Darrell Stokes, Ph.D.
Committee Member

Accepted:

_____
Lisa A. Tedesco, Ph.D.
Dean of the Graduate School

_____
Date

Translational Regulation of Kv4.2 in a Fragile X Mouse Model

By

Dan L. Pong
B.S., Emory University, 2009

Advisor: Gary J. Bassell, Ph.D.

An abstract of

A thesis submitted to the Faculty of the Graduate School of Emory University
in partial fulfillment of the requirements for the degree of Master of Science in Biology

2009

Abstract

Translational Regulation of Kv4.2 in a Fragile X Mouse Model

By

Dan L. Pong

Genetic ablation of the fragile X mental retardation protein (FMRP) results in fragile X syndrome (FXS), a mental retardation disorder associated with a high susceptibility to epilepsy. FMRP is expressed from the *FMR1* gene. FMRP is an mRNA binding protein crucial for local translation at synapses, suggesting that aberrant synaptic protein synthesis in the absence of FMRP might be the reason for compromised cognition and facilitated epileptogenesis. However, until now it is unclear if translational dysregulation of any specific target mRNA contributes to the epileptic phenotype of FXS.

A potential candidate is the potassium channel Kv4.2 which is fundamental for the regulation of neuronal excitability and, importantly, has been shown to be mutated in an inherited form of epilepsy. Preliminary data from the Bassell lab demonstrate that Kv4.2 mRNA associates with and might therefore be translationally regulated by FMRP. To test this hypothesis, I first analyzed dendritic Kv4.2 protein levels in brains from wild type and *Fmr1* knockout mice by immunohistochemistry and western blot analysis. With immunohistochemistry, I found significant downregulation of Kv4.2 protein in the *Fmr1* knockout. With western blot analysis, I found that dysregulation of Kv4.2 protein in the *Fmr1* knockout may be brain-region and cell-compartment specific.

To determine if Kv4.2 downregulation in the absence of FMRP is specific, I conducted similar experiments on potassium channels Kv1.2 and Kv3.4. Immunohistochemistry conducted on these proteins found no change in protein expression in the *Fmr1* knockout. I also conducted immunohistochemistry experiments on NMDA receptor subunit NR1, an mRNA known not to associate with FMRP. NR1 protein expression is not dysregulated in the *Fmr1* knockout. These data suggest that loss of FMRP does not cause a broad scale downregulation of ion channels and receptors. Furthermore, protein downregulation in the absence of FMRP may be dependent on FMRP-mRNA binding in wild type neurons. Using fluorescent *in situ* hybridization, I also found Kv4.2 mRNA localized in the dendritic fields in the hippocampus, suggesting a mechanism by which FMRP regulates neuronal excitability. My results suggest that Kv4.2 might be an important molecular determinant of FXS-related epilepsy.

Translational Regulation of Kv4.2 in a Fragile X Mouse Model

By

Dan L. Pong
B.S., Emory University, 2009

Advisor: Gary J. Bassell, Ph.D.

A thesis submitted to the Faculty of the Graduate School of Emory University
in partial fulfillment of the requirements for the degree of Master of Science in Biology

2009

Acknowledgements

I would like to thank all the people who have helped and inspired me during my masters work.

I would like to thank my advisor, Dr. Gary Bassell, for giving me the opportunity to explore neuroscience at the graduate level. His guidance and support for undergraduate research enabled me engage with science in such an in depth and exhaustive manner.

My post-doc Dr. Christina Gross deserves special thanks for the time she committed to me along the way. She showed me the ins and outs of sciences, training a simple biology major into a graduate-level neuroscience researcher.

I would like to thank Drs. Chen, English, Marsteller and Stokes for serving on my thesis committee. In particular, I'd like to thank Dr. Marsteller for her support and guidance. From supporting me as a SURE student researcher to our discussions about all things mentoring and thesis writing, Dr. Marsteller continually gave me great advising and mentoring which made my thesis possible.

To all my lab colleagues, thank you for giving me open access to a world of different ideas and cultures.

I would like to thank my friend Nathan Yogasundram; I came to Dr. Bassell's lab on his recommendation. Nathan was always there for me through thick and thin. He probably listened to every tale of mine of experiments gone awry. He was a true friend; he will be missed.

My deepest gratitude goes out to my family for their loving support throughout my life. My parents worked incredibly hard throughout their lives to give me the opportunity to learn at one of finest institutions in the country. They strongly supported my efforts to stay at Emory and attain this Masters degree. I thank my sister Ann for always reminding me that there is life beyond the lab, that a failed experiment is not the end of the world.

The generous support from the National Fragile X Foundation's William & Enid Rosen Summer Student Fellowship and Emory's SURE program was greatly appreciated. Without their support, I wouldn't have been able to devote a summer to full time research and learn what research truly entails.

Table of Contents

INTRODUCTION

Fragile X syndrome (FXS) is the most common form of inherited mental impairment (Penagarikano et al., 2007). This impairment can range from learning disabilities to more severe cognitive or intellectual disabilities, which are often referred to as mental retardation. FXS is the most frequent monogenetic cause of autism spectrum disorder. Fragile X syndrome is characterized by the absence of the fragile X mental retardation protein (FMRP), an mRNA binding protein which is encoded by the *FMR1* gene (Penagarikano et al., 2007). Although the underlying mechanisms are unknown, it is believed that FMRP plays a regulatory role in dendritic mRNA transport and local protein synthesis at synapses in neurons of brain areas involved in learning and memory (Figure 1) (Bassell and Warren, 2008).

Fragile X Syndrome Symptoms and History

The most prominent phenotype of fragile X syndrome is mental retardation, with IQ values typically between 20 and 70 (Fisch et al., 2002). The cognitive dysfunction particularly affects short-term memory for complex information, visuospatial skills and speech. A delay in speech is common and is often the first symptom that brings the child to medical attention. Epilepsy is another common symptom; it is reported to occur in 10 to 20% of individuals with fragile X syndrome (Berry-Kravis, 2002).

FXS is a sex-linked genetic disorder caused by the mutation of the *FMR1* gene on the X chromosome at band Xq27.3 (Harrison et al., 1983). Initially, researchers envisaged that FXS was a recessive X-linked condition. Later data from Sherman et al. disproved that model; the group demonstrated that 20% of males carrying the mutated *FMR1* gene were not affected (Sherman et al., 1985; Sherman et al., 1984). Furthermore, they

demonstrated that 30% of carrier females do exhibit some form of mental retardation. This created a paradox in which the genotype did not lead to a specific phenotype in all cases. Verkerk et al. resolved the paradox when they discovered a new inheritance model: trinucleotide expansion (Verkerk et al., 1991).

The Trinucleotide Expansion in Fragile X Syndrome: Full Mutations, Premutations and Associated Conditions

The trinucleotide expansion (CGG) for FXS is located in the 5' UTR of the *FMR1* gene. The repeat length is polymorphic and ranges from 6-54 CGG in normal individuals (Fu et al., 1991). Female carriers and normal carrier males show an expansion between 55 and 200 repeats, termed premutation. When the expansion exceeds 200 repeats, the repeats become hypermethylated and the *FMR1* gene is silenced; this is termed full mutation. No mRNA or protein is expressed from the silenced gene. The prevalence of the full mutation in the general population is estimated at 1/2364 for females who have at least one full mutation X allele and 1/3600 in males (Beckett et al., 2005).

Trinucleotide expansion syndromes are unique among genetic disorders because those without the full mutation may still have phenotypic mutations. Female FXS premutation carriers, who are cognitively normal, have a higher prevalence of premature ovarian failure (Penagarikano et al., 2007). Premature ovarian failure is defined as menopause before the age of 40; this condition is known as fragile X-associated primary ovarian insufficiency (FXPOI). Those with the premutation can also have a condition known as fragile X-associated tremor/ataxia syndrome (FXTAS). FXTAS symptoms include intention tremors and cerebellar ataxia at 50-60 years of age (Hagerman et al., 1994). Prior to onset, patients have normal cognitive ability. Both men and women can be

affected by FXTAS, although women show a later onset likely due to the degree of inactivation of the affected X chromosome (Hagerman et al., 2003). The prevalence of premutation alleles greater than 54 repeats in the general population is estimated at 1/259 in females and 1/813 in males (Rousseau et al., 1995). Unlike FXS, which is caused by loss of FMRP as a result of the full mutation, the premutation disorders FXTAS and FXPOI appear to occur from toxic gain of function from *FRM1* mRNA bearing excess CGG repeats (Oostra and Willemsen, 2009).

Fragile X Mental Retardation Protein (FMRP): mRNA binding and regulation

FMRP is an mRNA-binding protein that is found abundantly in neurons. It can act as a regulator of protein synthesis. FMRP has multiple mRNA binding domains that include two hnRNP-K homology domains (KH-domain) and one arginine rich RGG box (Figure 2). Based on microarray studies FMRP appears to associate with several hundred mRNAs, although most of these mRNA targets have not been validated (Bassell and Warren, 2008). Microtubule associated protein (MAP1b) and postsynaptic density protein 95 (PSD-95) are a few of the better characterized FMRP-targeted mRNAs (Lu et al., 2004; Muddashetty et al., 2007; Zalfa et al., 2007). The proteins encoded by these mRNAs play important functions in synaptic plasticity. PSD95 mRNA and another microtubule associated protein (MAP2) were shown to bind the RGG box of FMRP via a G-quartet stem-loop (Menon et al., 2008; Zalfa et al., 2007). Researchers posit that the G-quartet stem-loop is a common consensus sequence for a subset of FMRP mRNA ligands. Recently, Zalfa et al. reported a novel mRNA-binding domain in the N-terminus of FMRP (Zalfa et al., 2005). They suggest that this domain mediates binding to some mRNAs via a small, noncoding adapter RNA called BC1 (Tiedge et al., 1991).

Several studies have suggested that FMRP can act as either a positive or negative regulator for the protein expression of its ligands (Bechara et al., 2009; Lu et al., 2004; Muddashetty et al., 2007; Zalfa et al., 2003). Many groups have also shown that the absence of FMRP leads to the dysregulation of both basal and stimulus-induced synaptic translation (Dolen et al., 2007; Muddashetty et al., 2007; Weiler et al., 2004). A prevailing hypothesis within the field is that FMRP influences enduring forms of synaptic plasticity, e.g. learning and memory, by regulating local translation at synapses. In FXS, this translational control is abolished leading to severe impairments in neuronal function. In support of this theory, Muddashetty et al. (2007) demonstrated that the deletion of FMRP in mice results in dysregulated translation of specific target mRNAs at synapses.

Feng et al. demonstrated FMRP's role in healthy individuals (Feng et al., 1997a). They showed that normal FMRP associates with elongating polyribosomes within large mRNP particles. Feng et al. (1997a) also showed that a point mutation in FMRP, which was also shown to lead to FXS in humans (I304N missense mutation in the KH domain), leads to the incorporation into abnormal mRNP particles that are not associated with polyribosomes. This mutated FMRP still retains normal expression and cytoplasmic mRNA association. These data indicate that association of FMRP with polyribosomes must be functionally important and imply that the mechanism of the severe fragile X phenotype in the I304N patient lies in the sequestration of bound mRNAs into nontranslatable mRNP particles. Thus, the altered mRNA translation function of FMRP might be directly responsible for more severe development of FXS in individuals with the I304N missense mutation.

Fragile X Animal Model Studies

Several studies have validated the use of the *Fmr1* knockout mouse model for the study of many FXS characteristics. One of the hallmarks for the disorder's neuroanatomical phenotype in humans is the hyperabundance of dendritic spines with a long, thin, and otherwise immature morphology (Grossman et al., 2006; Irwin et al., 2000). Comery et al. demonstrated that the *Fmr1* KO mouse exhibits a similar excess of long, thin spines (Comery et al., 1997). *Fmr1* KO mice also display several neurological phenotypes observed in FXS patients such as altered learning and behavior, altered synaptic plasticity and greater susceptibility to seizures (Penagarikano et al., 2007).

Other FXS models have shown similar phenotypes reminiscent of FXS patients' characteristics. McBride et al. demonstrated that the deletion of *dfmr1* in *Drosophila melanogaster* leads to FXS characteristics such as abnormalities in spine morphology and behavior (McBride et al., 2005). Zhang et al. showed that an association demonstrated in the mouse model, FMRP with MAP1b mRNA (Lu et al., 2004; Zalfa et al., 2003), also occurs in *Drosophila* (Zhang et al., 2001). They used coimmunoprecipitation experiments to show the association between dFMRP and futsch, the MAP1b homolog. This suggests that the interaction of FMRP and at least one target mRNA is evolutionarily conserved.

Fragile X Syndrome and Epilepsy

As previously stated, about 25% of all FXS patients develop childhood epilepsy (Musumeci et al., 1999). As mentioned above, this phenotype is well-reflected in the FXS mouse model: *Fmr1* knockout mice have an unusually high susceptibility to audiogenic seizures and their neurons are hyperexcitable (Penagarikano et al., 2007). Several studies indicate that excessive signaling through group 1 metabotropic glutamate receptors (gp1 mGluRs) might cause at least some of the synaptic deficits in FXS (Penagarikano et al.,

2007). This reinforced the development of the mGluR theory of FXS (Bear et al., 2004). The mGluR theory of FXS (Figure 3) posits that many of the synaptic phenotypes in FXS can directly be attributed to exaggerated group 1 metabotropic glutamate receptor (gp1 mGluR) signaling, and therefore mGluR antagonists could be a useful therapy for FXS(Bear et al., 2004). Several studies show that a specific form of gp1 mGluR-dependent synaptic plasticity, mGluR-dependent long term depression (LTD), is enhanced in *Fmr1* knockout mice and occurs independently of protein synthesis (Huber et al., 2002; Nosyreva and Huber, 2006; Ronesi and Huber, 2008). mGluR-dependent long term depression (LTD) normally depends on protein synthesis, which is needed for the persistent internalization of AMPAR. These observations led to the hypothesis that FMRP normally acts as a negative regulator of translation downstream of Gp1 mGluRs; therefore the absence of FMRP leads to dysregulation of synaptic protein synthesis.

Studies have shown molecular associations of mGluR with epilepsy. Merlin et al. showed that the application of selective mGluR agonist (R,S)-3,5dihydroxyphenylglycine (DHPG) induces a gradual and persistent prolongation of epileptiform bursts in area CA3 of the hippocampus, similar to epileptic seizures (Merlin et al., 1998). More importantly, Chuang et al. demonstrated that those epileptiform discharges could be induced in *Fmr1*-KO mice without DHPG (Chuang et al., 2005). This data suggests that excess mGluR signaling plays a predominant role for the hyperexcitability of FMRP-deficient cells. In support of this theory, Yan et al. demonstrated that administration of MPEP (an mGluR5 antagonist) in a FXS mouse model reduces susceptibility to audiogenic seizures and abnormal open field behavior, two major phenotypes of the fragile X mouse (Yan et al., 2005).

Studies in *Drosophila melanogaster* and *Danio rerio* have shown similar recovery of morphologic, physiological, or behavioral impairments with administration of MPEP [2-methyl-6-(phenylethynyl) pyridine] (McBride et al., 2005; Tucker et al., 2006). Dölen et al. showed similar results in mice using a genetic reduction of mGluR signaling (Dolen et al., 2007). Dölen's group crossed *Fmr1* and *Grm5* (mGluR5 homolog) mutant mice to produce *Fmr1* knockout mice with a selective reduction of mGluR5 expression. These crossed-knockout offspring mice had reduced susceptibility to audiogenic seizures, less severe dendritic spine morphology defects and less severe protein synthesis in hippocampal slices as compared to *Fmr1* KO mice. Dölen et al. propose that these results suggest a direct correlation between translational impairment and the FXS phenotype. However, the precise molecular mechanisms that cause the hyperexcitability of FMRP-deficient neurons and may lead to epilepsy in humans have not been addressed so far.

Fragile X and Reduced Kv4.2 Function: a Potential Link to Epilepsy

An important mechanism to control excitability in healthy neurons acts via A-type currents mediated by voltage-gated potassium channels (Kv channels). A-type currents rapidly hyperpolarize cells in response to depolarization, thereby diminishing the back-propagation of action potentials into dendrites (Birnbaum et al., 2004). This controls the excitability of a neuron and regulates its capability to undergo long lasting changes in signal transmission. An important Kv channel regulating the hyperexcitability of neurons in the hippocampus is Kv4.2. This channel mediates transient A-type outward currents particularly in hippocampal dendrites. Kv4.2 is critically involved in the regulation of dendritic excitability and plasticity in the hippocampus, and a mutation in Kv4.2 has been linked to human temporal lobe epilepsy (TLE) (Chen et al., 2006; Singh et al., 2006).

The Kv channels are the mammalian gene counterparts for the *Shaker, Shab, Shaw,* and *Shal Drosophila* gene subfamilies of voltage-dependent K^+ channels. They play a crucial role during action potentials in returning the depolarized cell to a resting state. There are three groups of K^+ channels characterized based on the membrane topology of their principle subunits. In each case, the principle subunits tetramerize to form a single trans-membrane pore (Birnbaum et al., 2004). The first group, typified by voltage and Ca^{2+} activated K^+ channels, has six trans-membrane domains per α–subunit. The second group, typified by the "leak" K^+ channels, has four trans-membrane domains in their α–subunits. Lastly, the third group or "inward rectifiers" have two trans-membrane domains in each α–subunit (Birnbaum et al., 2004). A systematic nomenclature based on amino acid sequence of the α-subunits has been developed that defines *Shal* subfamily as Kv4.x (Birnbaum et al., 2004).

There are at least two examples showing that induction of an enduring increase of neuronal activity leads to reduced Kv4.2 function in the hippocampus in mice. NMDA-dependent long term potentiation of synapses leads to enhanced Kv4.2 channel internalization and epileptic seizures are accompanied by downregulation of Kv4.2 mRNA and protein levels (Birnbaum et al., 2004). In accordance, Chen et al. demonstrated that Kv4.2 knockout mice have a lower threshold for the induction of LTP in the CA1 region (Chen et al., 2006). Thus, a loss of functionality due to changes in Kv4.2 channels or the absence of FMRP both result in epilepsy.

Both Kv4.2 and FMRP have been linked to the modulation of spinal cord nociception through gp1 mGluR signaling (Hu et al., 2007; Price et al., 2007). These data suggest that Kv4.2 and FMRP function in the brain might be coupled. As a potential

mechanism, the Bassell lab posits that FMRP normally may act to stabilize mRNA and activate translation of Kv4.2. i.e. FMRP may halt the downregulation of Kv4.2 mRNA and protein that is triggered during epilepsy. This hypothesis was substantiated by preliminary data from the Bassell lab demonstrating that Kv4.2 mRNA associates with FMRP in cortical brain lysates (Figure 4). Furthermore, the Bassell lab has also shown that Kv4.2 protein is decreased in immunostainings on cultured *Fmr1* KO neurons (Figure 5). These data provide strong rationale to investigate a functional connection between FMRP and Kv4.2 in an *in vivo* study.

The goal of my project was to elucidate the potential molecular mechanisms underlying epilepsy in FXS. We hypothesize that downregulation of Kv4.2 mRNA and protein in the absence of FMRP is responsible for the FXS-characteristic neuronal hyperexcitability and, in some FXS cases, epilepsy. Thus, Kv4.2 dysregulation may be the key molecular determinant of FXS-related epilepsy. Analysis of the potential translational dysregulation of Kv4.2 in *Fmr1* KO mice may lead to the discovery of important mechanisms underlying epilepsy in FX patients, and suggest directions for therapeutic intervention.

MATERIALS AND METHODS

Materials:

Primary Antibodies:

- FMRP (rabbit polyclonal raised against the C-terminus of FMRP, generated in the Bassell lab) Used 1:100 in immunostainings.
- Kv1.2, clone K14/16; Neuromab (anti-mouse). Used 1:10000 in western blots and 1:1000 in mounted immunostainings.
- Kv3.4, clone N72/16; Neuromab (anti-mouse). Used 1:100 in western blots and 1:1000 in mounted immunostainings.
- Kv4.2, clone K57/1; Neuromab (anti-mouse). Used 1:250 in western blots, 1:2500 in mounted immunostainings, 1:5000 in free-floating immunostainings.
- Kv4.2, clone N-15; Santa Cruz (anti-goat). Used 1:200 in western blots and 1:250 in mounted immunostainings.
- MAP2, clone 5F9; Chemicon (anti-rabbit). Used 1:1000 in mounted immunostainings, 1:1000 in free-floating immunostainings.
- Tubulin, clone B-5-1-2; Sigma (anti-mouse). Used 1:200000 in western blots.

Secondary Antibodies:

- Donkey anti-goat IgG Cy-2 conjugated secondary antibody; Jackson ImmunoResearch Laboratories. Used 1:200 in mounted immunostainings.
- Donkey anti-goat IgG Cy-3 conjugated secondary antibody; Jackson ImmunoResearch Laboratories. Used 1:200 in mounted immunostainings.
- Donkey anti-goat IgG- Horseradish Peroxidase conjugated secondary antibody**;** Santa Cruz. Used 1:5000 in western blots.

- Donkey anti-mouse IgG Cy-2 conjugated secondary antibody; Jackson ImmunoResearch Laboratories. Used 1:200 in mounted and free-floating immunostainings.
- Donkey anti-rabbit IgG Cy-3 conjugated secondary antibody; Jackson ImmunoResearch Laboratories. Used 1:200 in mounted and free-floating immunostainings.
- Sheep anti-mouse IgG, Horseradish Peroxidase conjugated secondary antibody; ECL Western Blotting Detection Reagents from GE Healthcare, formerly Amersham Biosciences. Used 1:3000 in western blots.

Animals and tissue preparation

I used three week old *FMR1* knockout and WT littermates (B6.129P2-Fmr1$^{tm1Cgr/J}$, The Jackson Laboratory) in all experiments. Dr. Christina Gross (Bassell lab) perfused the mice transcardially with PBS followed by 4% paraformaldehyde (PFA; 4g Paraformaldehyde, 2.1g $Na_2H_2PO_4$, 100µl 1M $MgCl_2$, H_2O for total volume of 100ml, filtered) under deep anesthesia with pentobarbital sodium (150 mg/kg, i.p.) before removing the brain. The brains were stored in 4% PFA overnight at 4° C. I then transferred the brains to a 15% sucrose in phosphate-buffered saline solution (0.001M KH_2PO_4, 0.01M Na_2HPO_4, 0.137M NaCl, 0.0027M KCl, pH 7.0; aka PBS) and stored the brains at 4° C overnight. I froze the brains in Tissue-Tek using liquid nitrogen and stored the brains at -80° C.

Brain slice preparation for *in situ* hybridization/immunostainings

For the mounted *in situ* hybridizations and immunostainings, I cryostat-sectioned the brains into 10µm slices. The brains slices were stored at 4°C in 1xTBS (100mM Tris-

HCl, 150mM NaCl pH 7.5). I mounted one WT and KO brain slice each on Fisherbrand SuperFrost/Plus Microscope slides and stored the mounted sections at -80° C. For the free floating immunostainings, I cryostat-sectioned 40µm sections and stored them in 1x TBS at 4°C.

Antigen-retrieval, mounted immunohistochemistry

The sample slides were thawed at room temperature for 3-5min. I washed the slides twice in 1x TBS for 5min and then treated the samples with 0.8% sodium borohydride in 1xTBS for 10min. Afterwards, I washed the samples in 1x TBS and placed the slides in boiling citrate buffer (0.01M sodium citrate, pH 6.0). I heated the buffer inside the glass staining jar, containing the slide, to boiling in a microwave three times for 5min each at the lowest power setting. Afterwards, the slides cooled on the bench top at room temperature for 30min. I washed the samples in 1x TBS for 5min and then permeabilized them using 0.5% Triton X-100 in 1x TBS. Samples were incubated in 10% normal donkey serum, 0.1% Triton X-100 in TBS for 1hr at room temperature before applying the primary antibodies, which were diluted in antibody solution (2% donkey serum, 0.1% Triton X in TBS); see antibody section at end of materials for concentration. Afterwards, the samples were covered in plastic cover slips (Hybri-slips; Sigma-Aldrich) and incubated overnight at room temperature in a humid chamber. Slides were then washed three times in 1x TBS for 10min. Then I applied the secondary antibodies (dilution 1:200) in antibody solution and incubated the slides for 1-2hr at room temperature, protected from light. Lastly I washed the slides three times in 1x TBS for 10min, rinsed the slides in ddH_2O and mounted the slides with mounting medium (100ml

1xPBS, 25g polyvinyl alcohol, 50ml glycerol; pH 7.2) beneath glass cover slips (Corning Glass).

Free-floating immunohistochemistry

I placed the sections in 12-well tissue culture plates (BD Falcon) and washed them four times in 1x TBS for 5min. The tissue was denatured and rehydrated in a graded alcohol series for 5min in each stage: 10% Ethanol (EtOH) in 1xTBS, 20% EtOH in 1xTBS, 40% EtOH in 1xTBS, Methanol-Acetone (1:1), 40% EtOH in 1xTBS, 20% EtOH in 1xTBS, 10% EtOH in 1xTBS. Afterwards, I washed the samples three times in 1x TBS for 5min. Then I washed the samples in 0.3% Triton X-100 in 1xTBS for 30min before preincubating the samples in 10% normal donkey serum and 0.1% Triton X-100 in 1xTBS. Afterwards, I applied the primary antibodies (see antibody section for concentrations) in antibody solution over night at room temperature. The next day, I washed the samples four times in 1x TBS for 10min. After washing, I incubated the samples for 2hr in secondary antibody (1:200 in antibody solution) and then washed the samples four times in 1x TBS for 5min. The sections were mounted on SuperFrost/Plus slides and left to air-dry. Lastly, I covered the sections in mounting media and covered them with glass cover slips.

Fluorescence *in situ* hybridization

We obtained the rat sequence (covering the 5'UTR and parts of the open reading frame [nt 1-860 in pBluescript]) from Dr. Andreas Jeromin (Allen Institute for Brain Science). Dr. Gross amplified and cloned the mouse cDNA: nt 1759-2112 of Kv4.2 encoding the opening reading frame in pcDNA3 plasmid.

Preparation of DIG-labeled Probe

All buffers were prepared and cooled them to 4° C before starting the protocol. I linearized 10µg of the plasmid cDNA (see below). I ran a sample of the probe on an agarose gel to ensure linearization (see below). Afterwards, I raised the volume of the sample to 100µl with H_2O and removed the protein using phenol-chloroform extraction (see below). The linearized plasmid was *in vitro* transcribed with a DIG RNA Labeling Kit (SP6/T7; Roche), according to the manual. The samples were incubated with RNA-free DNAse for 15min at 37° C to remove the template. Afterwards, I raised the volume to 50µl total volume with fresh ddH_2O and took a 3µl sample for an analytic RNA gel (see below). The unincorporated nucleotides were removed using illustra MicroSpin™ G-25 Columns, according to the manual. To the sample, I added 50µl H_2O, 20µl 3M sodium acetate ($NaCH_3COO$), pH 5.2; 10µl yeast t-RNA (10mg/ml) and 300µl EtOH. The samples were incubated for an hour at -20° C. I spun down the samples for 15min at 20000g & 4°C, removed the ethanol from the samples and air-dried the tubes for 20min at 37° C. Probes were then dissolved in 160µl of 0.1M DTT.

DNA Plasmid Linearization

Dr. Gross provided the bacterial plasmids containing mouse Kv4.2 (pcDNA3), rat Kv4.2 (pBluescript II KS+) and Arg3.1 (open reading frame pcDNA3). I prepared the following mixture for each plasmid: 15µl of 1µg/µl plasmid DNA, 4µl of restriction enzyme, 5µl of 10x Fast Digest buffer (Fermentas) and 26µl of H_2O. Xho1 and HindIII restriction enzymes were used for mouse Kv4.2 antisense and sense riboprobe generations, respectively. ApaI restriction enzyme was used for rat Kv4.2 riboprobe generation. Xho1 and EcoR1 restriction enzymes were used for Arg3.1 antisense and

sense riboprobe generations. I vortexed the mixtures and incubated the samples overnight at 37° C.

DNA Gel Electrophoresis

From the 50µl samples of DNA linearized over night, I took 2µl to run a test DNA gel. To the restriction sample, I added 0.5µl of enzyme and incubated the mixture for an hour. I prepared a 0.8% agarose gel and supplemented it with 0.1µg/ml ethidium bromide in TAE (1x Tris-Acetate EDTA buffer (0.04M Tris-Acetate, 0.01M EDTA, 0.02 Glacial Acetic Acid, pH 8.4). To 2µl linearized plasmid sample, I added 2µl of 6x DNA loading dye and 8µl of H_2O. As control, 0.5µl of uncut sample was added to 9.5µl H_2O and 2µl 6x DNA loading dye. I vortexed the 12µl mixtures, spun them down, and loaded them onto the gel. 1x TAE was used for the running buffer. I ran the gel at 90mV using a PowerPac 200 (Bio-Rad) power supply and visualized the DNA bands with UV light. When the plasmid linearization was complete (Figure 6), I removed the restriction mixture from the 37° C incubator, stopping the restriction reaction. I purified the DNA by phenol-chloroform extraction.

Phenol-chloroform extraction

To the linearized DNA, I added H_2O to raise the sample volume to 100µl. Next, I added 100µl of phenol-chloroform, vortexed the samples and centrifuged them at 20,000g and 4°C for 10min. After centrifugation, two phase separate phases were visible. I pipetted off the upper aqueous phase and added 100µl of chloroform to it to remove any remaining phenol. I vortexed the samples and centrifuged them at 20,000g and 4°C for 10min. The aqueous phase was pipetted off into new tubes. In the new tubes, I added 10µl of 3M sodium acetate, pH 5.2 and 250µl 100% EtOH to the samples to precipitate

the DNA. The samples were vortexed and chilled at -20°C for half an hour. Afterwards, I centrifuged at 20,000g and 4°C for 20min. The supernatant was removed, and the pellet was washed with 1ml of 75% EtOH. I vortexed the samples and spun them down at 20,000g and 4°C for 5min, removed, and let the tubes air-dry for 5-10min. I resuspended the pellet in 15µl ddH_2O and then ran a DNA gel electrophoresis to ensure DNA linearization after phenol-chloroform extraction (Figure 7).

RNA Gel Electrophoresis

I prepared a 1.2% agarose gel and supplemented it with 7.5ml Formaldehyde and 5ml 10x MOPS buffer (0.2M MOPS, 20mM sodium acetate, 10mM EDTA). I prepared an RNA sample buffer with 100µl formamide, 20µl MOPS, 30µl formaldehyde, and 1µl ethidium bromide. To 9µl of the sample buffer, 3µl of RNA sample or 3µl RNA ladder was added. I heated the RNA mixtures to 65°C for 15min and then put them on ice to denature the RNA. DNA loading buffer was added to the mixtures and the samples were loaded on to the gel. 1x MOPS was used as the running buffer. I ran the gel at 90mV using a PowerPac 200. RNA bands were visualized with UV light (Figure 8).

Probe-size reduction

To the 160µl of probe RNA, I added 20µl of 0.4M $NaHCO_3$ and 0.6M Na_2CO_3. The probe mixture was mixed and incubated at 60° C for a period of time based on the original and final (0.1 kb) sample length. I stopped the reduction reaction by adding 7µl of neutralizing salt (3M sodium acetate, pH 6.0). I then added 2µl 10mg/ml glycogen, followed by 500µl EtOH to precipitate the RNA. The size-reduced-probe mixture was vortexed, incubated on ice for 30min and spun down for 15min at 4° C. I rinsed the pellet with 70% EtOH and air-dried it. I then dissolved the pellet in 10µl fresh ddH_2O and

added 50µl of hybridization buffer [10ml 20xSSC; 25ml formamide; 0.5ml 100x Denhardts; 10ml dextrane sulphate (50%); 2.5ml herring sperm ssDNA (10mg/ml); 0.5ml yeast-tRNA (25mg/ml)]. I did a dot blot test to verify DIG-UTP incorporation as well as check the concentration of the riboprobes (Figure 9); see below for protocol.

Dot Blot

I applied control labeled RNA to the Zeta-Probe Blotting Membrane (Bio-Rad) in 10ng, 5ng, 2.5ng and 1.0ng amounts, as well as 1:10, 1:20, 1:40, and 1:100 dilutions of the riboprobes. The membrane was UV-crosslinked (2x 125kJ) using a GS Genelinker (Bio-Rad). I briefly rinsed the membrane in washing buffer (0.1M maleic acid, 0.15M NaCl, pH 7.5; 0.3% (v/v) Tween 20) and incubated the membrane for 30min in blocking solution (0.1M maleic acid, 0.15M NaCl, pH 7.5; 0.5% blocking reagent (Roche)). Afterwards, I incubated the membrane for 30min in antibody solution (Anti-Digoxigenin-AP Fab fragments, 1:2500 in blocking solution). I then washed the membrane twice for 15min each in washing buffer. Next, the membrane was equilibrated for 2-5min in detection buffer (0.1M Tris-HCl; 0.1M NaCl, pH 9.5). I incubated the membrane in freshly prepared color substrate solution [1 NBT/BCIP Ready-to-Use Tablet (Roche) in 10ml detection buffer] in a covered container. After the desired spot/band intensities were achieved, I stopped the reaction with 50ml ddH_2O (Figure 9).

Preparation of Slides

First, I prepared all of the solutions and chilled them down to 4° C. The slides were thawed and air-dried at room temperature. I fixed the slides in 4% PFA for 5min., washed the slides twice for 10min in 2x SSC (0.6M NaCl, 0.06M sodium citrate, pH 7.0) and then incubated them with 0.1M triethanolamine-HCl (TEA), pH 8.0. I added 1.25ml

of acetic anhydride to 100ml 0.1M triethanolamine, pH 8.0 (cold) while stirring. The slides were then immediately placed into TEA/acetic anhydride solution and incubated for 10min. Afterwards, I washed the slides in ddH_2O three times and incubated the slides in acetone and methanol (1:1). I washed the slides twice more in 2x SSC for 10min. I applied hybridization buffer to the slides and placed them in a wet chamber to incubate for 1-2hr at room temperature.

Hybridization of slides

I thawed the riboprobes on ice and diluted them in hybridization buffer to a final concentration of 1-10ng/µl. The riboprobes were denatured at 90° C for 5min and then immediately put on ice. I removed the hybridization buffer from the slides and added 50-100µl of hybridization mixture per slide. The slides were covered with plastic cover slips and incubated in a humid chamber for 18hrs at 55° C.

Washing

Slides were washed twice in 2x SSC for 10min and were then incubated at 37° C with 10µg/ml RNase A in 2x SSC (preheated to 37° C) for 15min. I then washed the slides twice in 2x SSC for 10min and once in 0.5x SSC for 5min at room temperature. Then I washed the slides once in 0.5x SSC at 56° C for 30min, twice in 2x SSC for 10min and incubated them in 2% H_2O_2 in 1x SSC for 15min. Afterwards, I washed the slides three times in 1x SSC for 5min. Finally, I washed the slides once in 1x TBS for 5min.

Detection with TSA-Plus Fluorescein System

After washing, the slides were blocked in TNB buffer (0.1M Tris-HCl, pH 7.5; 0.15NaCl; 0.5% blocking reagent, Roche) for 30min at room temperature and incubated

in anti-digoxigenin-POD, Fab Fragments (Roche) for 2hr in blocking buffer. Afterwards, I washed the slides five times in TNT buffer (0.1M Tris-Hcl, pH 7.5; 0.15M NaCl; 0.05% Tween20) for 5min and then incubated the slides in tyramide amplification reagent working solution [Tyramide Signal Amplification- Plus Fluorescein System (Perkin-Elmer)] at room temperature in a covered chamber for 10min. I washed the tyramide-amplified slides five times in TNT buffer in a covered glass staining jar for 5min. and later rinsed the slides in H_2O and air-dried them. I applied mounting media to the sections and mounted the slides under glass cover slips. The slides were air-dried and then placed in -20° C for storage.

SDS-polyacrylamide gel electrophoresis (SDS-PAGE), protein transfer and western blot

I prepared an 8% running gel with a 6% stacking gel as described in *Molecular Cloning* (Sambrook et al., 2001). We loaded the samples on the gel and ran the gel at 100mV until the blue dye in the loading buffer reached the bottom of the gel. For the protein transfer to a PVDF-membrane (Bio-Rad), I incubated the gel in transfer buffer [200ml methanol, H_2O to raise volume to 900ml, 100ml Tris-glycine (25mM Tris, 192mM glycine, pH 8.3)] for 15min. Meanwhile I briefly rinsed the membrane in methanol, briefly in H_2O and finally in transfer buffer for 5min. The protein samples were transferred from gel to membrane in a Mini Trans-Blot cell (Bio-Rad), using a PowerPac 200 at 100mv for 75min. Afterwards, I briefly rinsed the membrane in methanol and dried it on Whatman paper. Next I washed the membrane in methanol for 5min before placing it in blocking solution (5% powdered skim-milk in PBS-T) for 1hr. I then washed the membrane three times in PBS-T (PBS supplemented with 0.1%

Tween20) for 5min. The primary antibodies (see antibody section for concentrations) were diluted in PBS-T and incubated on the membrane at 4°C overnight. The next day I washed the membrane three times in PBS-T for 10min and incubated it in secondary antibodies coupled to horseradish peroxidase (see antibody section for concentrations) in PBS-T for an hour. Afterwards the membrane was washed three times in PBS-T again. To detect the antibody staining, a chemiluminescence substrate (SuperSignal, ThermoScientific) was used. I incubated the membrane in SuperSignal for 5min. Using forceps, I removed the membrane from the western blot box and blotted the excess substrate solution on a paper towel. The membrane was exposed to light-sensitive films (CL-X Poser Film, ThermoScientific) for different times (1-30min) in an autoradiography cassette. I scanned the films and analyzed the data as described. If the membrane was reprobed for additional antibodies, it was first incubated with 10ml of Restore Western Blot stripping buffer (Thermoscientific) at 37° C for 20min. I then washed the membrane three times for 10min after stripping, blocked and incubated the primary antibodies as described above.

Synaptoneurosome and protein sample preparation for SDS-PAGE

After sacrificing the mice and removing the brains, Dr. Gross and I dissected the mid-brain, white matter and blood vessels from the brains. We then homogenized the brains with a mortar and pestel in homogenization buffer (118 mM NaCl, 4.7 mM KCl, 1.2 mM $MgSO_4$, 2.5 mM $CaCl_2$, 1.53 mM KH_2PO_4, 212.7 mM glucose, and 1 mM DTT, pH 7.4, supplemented with RNAse- and proteinase-inhibitors). We saved 100µl of sample for the "total homogenate samples" and the rest we filtered through 3 layers of 100µm-pore nylon membranes. We then filtered the samples through 2 layers of 11µm-

pore nylon membranes. Equal amounts of 2x loading dye were added to the total lysate and synaptoneurosome preparations. We boiled the samples at 95° C for 5min and then either ran the samples on an SDS-PAGE gel immediately, or stored them at -20° C.

Data Analysis

Imaging of FISH and Immunostainings: I scanned the images using a Zeiss LSM510 Meta confocal microscope and deconvolved the images with AutoQuant X software (Media Cybernetics). I quantified the signal intensities using Imaris suite software (Bitplane). Signal intensities were measured from deconvolved z-stacks as mean intensity per volume, in the molecular layer (dendrites) of the dentate gyrus and the stratum radiatium (dendrites) of the CA1 region (Figure 13). I collected data for at least three different brains for each genotype (WT and KO) and condition. These brains were analyzed paired, i.e. WT and KO were mounted on the same microscope slide for immunohistochemical analyses. Data from *Fmr1* KO was normalized to the WT control. With these data sets, I performed paired t-tests to analyze for significant differences between WT and KO. Error bars reflect the standard deviation.

Quantification of western blots: I scanned the films and measured signal intensities of specific bands using ImageJ software. The signal intensities were expressed as mean signal intensity per area. Total lysates or synaptic fractions from WT and KO littermates or age-matched WT and KO pairs were always analyzed on the same protein gel. I normalized the intensities of Kv4.2 and other ion channels to Tubulin specific bands. Data were collected from at least three different brains for each genotype and paired t-tests were conducted to determine any significant differences between WT and KO.

RESULTS

The aim of this project was to determine the effects of *Fmr1* gene ablation on the protein expression of the voltage-gated potassium channel Kv4.2 in dendritic fields of the dentate gyrus and CA1 regions of the mouse hippocampus. To achieve this goal, I analyzed Kv4.2 protein expression using both histological and biochemical methods. I also studied the effects of *Fmr1* ablation on other voltage-gated potassium channels and a NMDA receptor subunit to determine the specificity of the observed effects. Raab-Graham et al. demonstrated that Kv1.1 is translated locally in dendrites (Raab-Graham et al., 2006). Given the homology of Kv channels, Kv4.2 mRNA may also undergo local translation in dendrites similar to Kv1.1. Muddashetty et al. proposed that one of FMRP's regulatory functions is mediating local translation of target mRNAs in dendrites (Muddashetty et al., 2007). Thus if Kv4.2 mRNA is found to undergo translation locally in dendrites, FMRP may act as the regulatory protein. In order to study a potential role of FMRP on Kv4.2 mRNA dendritic localization and/or synaptic translation, I analyzed Kv4.2 mRNA localization within the hippocampal neurons.

Kv4.2 protein is downregulated in dendritic areas of the Fmr1 KO hippocampus

To determine protein levels in the hippocampus, I undertook immunostainings on cryostat- sectioned mice brains. Using Kv4.2 antibodies from Neuromab and Santa Cruz, I performed immunostainings on slides mounted with both WT and KO brain sections. Using the Neuromab antibody, immunoreactivity to Kv4.2 protein was reduced 26% in the dentate gyrus of KO mice relative to WT controls (Figures 14,15). Using the Santa Cruz antibody, only a non-significant 13% difference was found in the KO dentate gyrus (Figures 16,17). I further quantified Kv4.2-specific signal in the dendritic fields of the CA1 (stratum radiatum). Using the Neuromab antibody, immunoreactivity to Kv4.2

protein was reduced 28% in the KO (Figures 14,15) while using the Santa Cruz antibody immunoreactivity to Kv4.2 protein was reduced 21% in the KO (Figures 16,17). The finding that two different Kv4.2 antibodies show reduced immunoreactivity in the absence of FMRP is an important corroboration of our initial hypothesis that Kv4.2 protein expression might be downregulated in FXS.

My initial experiments were conducted on mounted brain sections. I later tried free floating immunostainings with the hope of better antibody penetration. Prior experiments in the Bassell lab demonstrated the technique's validity (Bassell – unpublished). Free-floating immunostainings have the advantage of having both sides of the brain section exposed to antibodies while mounted section only have one face exposed. Thus we anticipated the free-floating protocol would produce more accurate results. After several attempts to optimize the free-floating immunostaining protocol for quantification purposes, we determined that the mounted immunostainings were more consistent and reproducible than the free-floating staining. Consequently my data shown reflects the mounted immunostaining experiments. Given that brain slices have no structural support in free-floating staining, I had to use thicker slices (40μm) than were used in the mounted experiments (10μm). Analysis of z-sections of free-floating brain sections showed strong antibody signal on the opposing faces of the brain slices but little signal towards the middle. Furthermore, I could not use the antigen-retrieval protocol used for mounted sections with the free-floating sections, as it destroyed the slices' morphology. Antigen-retrieval breaks up protein cross-links, exposing more antigen and increasing antibody signal intensity.

Initially, we attempted to normalize Kv4.2 signal to MAP2, a dendritic marker (Figure 12). The MAP2 antibody had been shown to be a strong marker of dendritic localization in cell culture experiments (Bassell – unpublished). However, MAP2 staining was inconsistent; MAP2 staining varied widely even within brain slices from the same animal. Thus it was not a good normalization standard for quantification. Therefore, we increased the number of experiments and quantified Kv4.2 signal intensity without normalization to MAP2.

NR1 protein is not downregulated in the Fmr1 KO hippocampus

To test the specificity of the Kv4.2 results, I also analyzed the hippocampal protein expression of NR1, a subunit of the ligand-gated calcium channel NMDA receptor, which is unrelated to the Kv protein family. Preliminary data indicated that NR1 mRNA is not associated with FMRP (Figure 4, Bassell – unpublished). We therefore anticipated that NR1 expression is not affected by the absence of FMRP. As expected, NR1-specific immunostainings in dendritic fields of the dentate gyrus and CA1 showed no significant change in NR1 expression between WT and KO brains (Figures 18,19). This suggests that NR1 is not regulated by FMRP and furthermore that not all classes of receptors and channels are downregulated in the absence of FMRP.

Kv1.2 and Kv3.4 protein are not downregulated in dendritic areas of the Fmr1 KO hippocampus

To investigate whether other voltage-gated potassium channels are downregulated within dendritic fields of the *Fmr1* KO hypocampus I analyzed the protein expression of the voltage-gated potassium channels Kv1.2 and Kv3.4 by immunostainings. Kv1.2 and Kv3.4 have different functions than Kv4.2 during the generation of a neuronal action

potential and thus may or may not be involved in FXS-related hyperexcitability. Using antibodies from Neuromab, I demonstrated that there is no significant change in Kv1.2 and Kv3.4 protein expression in the dendritic fields of the dentate gyrus and CA1 region of the *Fmr1*-KO mouse. Immunostainings on KO sections showed a 4% increase in the DG and a 7% increase CA1 of Kv1.2 that were not statistically significant (Figures 20,21). Kv3.4 demonstrated 9% and 11% reductions in the DG and CA1, respectively, in the knockout; these changes were also not significant (Figures 22,23). This suggests that Kv1.2 and Kv3.4 protein expression is not regulated by FMRP and further strengthens the hypothesis that Kv4.2 might play a key role in FXS-related epilepsy.

Biochemical probing of voltage-gated potassium channels

To alternatively investigate ion channel expression, I conducted western blot experiments on brain lysates and synaptoneurosomal preparations of hippocampal lysates. The brain (total) lysates contained cortex and hippocampi. Synaptoneurosomes are preparations of highly enriched, pinched-off synaptic compartments (Figure 24). Synaptoneurosomes retain normal functions of neurotransmitter release, receptor activation, and various postsynaptic responses including signaling transduction and protein synthesis. Using both Kv4.2 antibodies, I found no significant change in protein expression in the *Fmr1* KO brains in either total or synaptoneurosome preparations (Figures 25-28).

We hypothesize that the differences in immunostainings and western blot analysis can be attributed to the nature of cell types studied in each technique. In the western blots, the total brain lysates include all sections of the cortex and hippocampus as well as all cell types and sections. Consequently, they reflect the Kv4.2 expression of passing

interneurons, cell bodies and dendrites as opposed to the dendritic-specific regions of the hippocampus tested in the immunostainings. In the synaptoneurosome preparations, the synaptic compartments may still be from outside the region of interest studied in the immunostainings. Furthermore, the synaptoneurosomes do not include dendritic shafts, and may therefore not include enough dendrite length to be representative of the region studied in the immunostainings.

I also tested Kv1.2 and Kv3.4 proteins using western blot analysis. As suggested by the immunostainings, I found no changes in protein expression in the *Fmr1* KO mouse in either total or synaptoneurosome preparations (Figures 29-32).

Analysis of Kv4.2 mRNA suggests localization in hippocampal dendrites

Kv1.1, another voltage-gated potassium channel, was shown to undergo local translation in hippocampal dendrites (Raab-Graham et al., 2006). To investigate whether Kv4.2 mRNA translation might be also regulated locally at synapses, I conducted Kv4.2-specific fluorescence *in situ* hybridization (FISH) experiments on the same regions tested in the immunostainings as well as in the cortex. I generated antisense mRNA strands (riboprobes), as described in the methods section, and applied them to sections of the same WT and KO brains used in the immunostaining experiments. In both the WT and KO brains, probing with Kv4.2 antisense riboprobes showed Kv4.2 mRNA localization in the dendrites of the CA1, dentate gyrus and cortex regions of the brain (Figure 33). High background staining made absolute identification of Kv4.2 mRNA localization difficult.

Antisense riboprobes specific to the immediate early gene Arc/Arg3.1 were generated as a positive control (Figure 34), because Arc/Arg3.1 mRNA is localized to

dendrites and has a characteristic expression pattern in the dentate gyrus (Link et al., 1995; Lyford et al., 1995). The sense riboprobes for both Kv4.2 and Arc/Arg3.1 showed no specific signal above background levels (example for Arc/Arg3.1 sense probe shown in Figure 34).

Initially I used antisense and sense Kv4.2 riboprobes derived from the rat sequence, which showed little signal specificity over background in either the WT or KO sections. This may be due to the differences between the rat and mouse sequences of Kv4.2. To improve signal specificity, I generated new mouse Kv4.2 riboprobes, which showed specific signals. In general, Kv4.2-specific FISH signals were weak and showed a low signal-to-noise ratio. To enhance intensity of Kv4.2-specific signals, I used tyramide amplification (Bobrow and Moen, 2001). I also altered several variables of the FISH protocol in order to optimize signal to noise ratios.

The riboprobes were all size-reduced because smaller fragments of RNAs were shown to have improved accessibility to target mRNAs in the tissue. The size-reduced Kv4.2 riboprobes were tested against non-size reduced Kv4.2 riboprobes generated in the same *in vitro* transcription experiment. The size-reduced riboprobes displayed greater signal specificity than the non-size-reduced probes (data not shown). Further optimization attempts to reduce the high levels of background staining (see Figure 33), by e.g. using different probe-reduction lengths, did not improve the staining specificity.

CONCLUSIONS AND DISCUSSION

In this project, we sought to test the hypothesis that the protein expression of voltage-gated potassium channel Kv4.2 in dendrites and at synapses may be dysregulated in the absence of FMRP, and thus might be the key underlying molecular cause of fragile X syndrome-related epilepsy. Using immunofluorescence staining, I showed that Kv4.2 protein is downregulated in *Fmr1* KO mice in key areas of the hippocampus known to be involved in epilepsy. In contrast, I found that protein expression of other voltage-gated potassium channels (Kv1.2 and Kv3.4) remains unchanged in wild type and knockout. These data corroborate our hypothesis that Kv4.2 expression is specifically dysregulated in FXS and thus might an important molecular determinant for FXS-related epilepsy. Furthermore my studies on the NMDA receptor subunit NR1, an mRNA known not to associate with FMRP, suggest that the loss of FMRP does not cause a broad scale downregulation of ionotropic channels and receptors in the brain. Although I detected significant downregulation of Kv4.2 via microscopy methods, I was unable to reproduce these results with western blot analyses on total and synaptic brain fractions. As a possible explanation, we suggest that the western blot assays may not be as specific as our microscopy methods. Consequently, the Kv4.2 downregulation seen in the immunostainings may be a brain region and cell-compartment specific occurrence (as discussed in results section). Using signal-enhanced fluorescent in situ hybridization, I demonstrate that Kv4.2 mRNA may localize in the dendritic fields of the hippocampal areas CA1 and dentate gyrus. This suggests that Kv4.2 might be translated locally at synapses. Local translation of Kv4.2 may account for the above mentioned region and cell-compartment specificity of Kv4.2 downregulation in the absence of FMRP.

Downregulation of Kv4.2 protein in hippocampal dendrites of Fmr1 KO mice

The downregulation of Kv4.2 protein in *Fmr1* KO mice suggests that FMRP is involved in Kv4.2 protein expression. Although the specific molecular mechanisms of this downregulation are unknown, the observation itself suggests a mechanism linking fragile X syndrome to the epilepsy seen in 25% of FXS patients.

Several labs have suggested mechanisms of action of FMRP on mRNA to explain protein expression dysregulation in *Fmr1* KO mice. Lu et al. suggest that FMRP interaction with MAP1B mRNA leads to polysomal stalling and consequently halts translation of MAP1B mRNA (Lu et al., 2004). Darnell et al. suggest that FMRP/mRNA binding leads to the retention of mRNAs in translationally inactive messenger RNPs (mRNPs) via its interaction with a complex secondary structure called "kissing complex" mRNA motif, and that this association is disrupted by the I304N point mutation (Darnell et al., 2005). In contrast, Bechara et al. propose that *Sod1* mRNA is translationally activated by FMRP via a novel mRNA motif, SoSLIP (*Sod1* mRNA stem loops interacting with FMRP) (Bechara et al., 2009).

A point of contention in the literature is when and how FMRP exerts its regulatory functions. Darnell et al.'s (2005) model proposes that FMRP association with polysomes is mediated by mRNA ligands (via the kissing complex). Conversely, Napoli et al. propose that a binding partner of FMRP, CYFIP1/Sra1, directly binds to translation initiation factor eIF4E, repressing translation initiation (Napoli et al., 2008). They, therefore, propose CYFIP1/Sra1 as a novel 4E-binding protein (4E-BP). 4E-BPs are a class of translational inhibitors and important regulators of overall translation initiation in cells. By binding eIF4E, 4E-BPs impair recruitment of the 40S ribosomal subunit to the

cap structure present at the 5′-end of all eukaryotic cellular mRNAs (Teleman et al., 2005). Napoli et al. hypothesize that FMRP interactions with CYFIP may regulate translation initiation by keeping the mRNP complex dormant until activation by signaling downstream of cell surface receptors (Napoli et al., 2008).

Several studies suggest that particular FMRP/mRNA-binding motifs are responsible for certain types of protein dysregulation. The Jan group showed that *Sod1* mRNA has a FMRP binding motif (SoSLIP) that acts as a translational activator in the presence of FMRP (Bechara et al., 2009). Other groups suggest that the G-quartet and "kissing complex" mRNA motifs serve as translational inactivators (Lu et al., 2004; Muddashetty et al., 2007). The location of the mRNA binding motif might be as important a determinant of mRNA regulation as the motif sequence motif itself. A G-quartet motif found in the 3' UTR region of PSD95 mRNA has been shown to act as a translational inhibitor in the presence of FMRP (Muddashetty et al., 2007). Zalfa et al. suggested that the G-quartet motif within the 3' UTR of PSD95 mRNA mediates FMRP-regulated mRNA stability (Zalfa et al., 2007). In an FMRP unrelated study, Hüttelmaier et al. demonstrated that Zipcode binding protein 1 (ZBP1) binds to the 3' UTR of β-actin mRNA (Huttelmaier et al., 2005). They found that the binding region (zipcode) in the 3' UTR of β-actin mRNA also serves as a translational inhibitor, a function similarly seen in FMRP/PSD95 mRNA binding. Conversely, motifs in the 5' UTR have been shown to serve as translational activators. Cho et al. demonstrated that the internal ribosomal entry site (IRES) RNA motif of BiP mRNA is located in the 5' UTR and serves as a translational activator in the presence of Synaptotagmin binding, cytoplasmic RNA interacting protein (SYNCRIP)(Cho et al., 2007). SoSLIP, the FMRP binding motif

described by the Jan group, was proposed to be a translational activator located in the 5' UTR of Sod1 mRNA (Bechara et al., 2009). These observations all support the idea that the mechanisms mRNA motifs' regulatory function may depend on the location of the particular binding motif.

We expect that determining the binding site of FMRP and Kv4.2 mRNA would clarify the regulatory roles FMRP has for Kv4.2 mRNA and protein. Currently, the Bassell lab is attempting to analyze this association in more detail using co-immunoprecipitation experiments with FMRP and Kv4.2 mRNA deletion constructs. If successful, these experiments will demonstrate the location of the FMRP-binding motif as well as the FMRP-binding sequence. The Kv4.2 reduction seen in the absence of FMRP suggests that FMRP acts as a translational activator of Kv4.2 mRNA in wild type as suggested for *Sod1* mRNA (Bechara et al., 2009). However, by *in silico* analysis, I could not detect any SoSLIP-like motifs within Kv4.2 mRNA.

One important preliminary experiment is to show a direct interaction of Kv4.2 mRNA and FMRP. Electrophoretic mobility shift assays (EMSA) could be used to address this question. An EMSA is the electrophoretic separation of a mixture of purified recombinant protein and DNA or RNA on a polyacrylamide or agarose gel. Based on size and charge differences, a protein-RNA complex will travel through a gel slower than unbound protein. Additionally, cross-linking experiments could be used to analyze for direct interactions. In this experiment, protein lysates from tissue or cells are chemically cross-linked to generate covalent binding between protein and RNA molecules which interact directly. After cross-linking, lysates will be treated with an ionic detergent such as sodium dodecyl sulfate (SDS) to eliminate any noncovalent associations. Then, the

protein of interest (i.e. in this case FMRP) is precipitated using a specific antibody. The protein-RNA complexes are then separated again by reversing the cross-linking. The identity of the associated RNAs can then be determined by reverse transcriptase PCR (RT-PCR).

Kv4.2 downregulation in the absence of FMRP is specific

My data suggests that the protein downregulation seen with Kv4.2 might depend on the association of FMRP with Kv4.2 mRNA. Preliminary data from the Bassell lab demonstrated that Kv4.2 mRNA could be co-immunoprecipated with FMRP. This was similar to PSD95 mRNA, another putative target of FMRP. Conversely in this experiment NR1 mRNA, which encodes a subunit of NMDA receptors, did not associate with FMRP (Figure 4). I showed that protein expression of NR1 in the *Fmr1* KO mice was unchanged, suggesting that the role of FMRP for protein expression depends on its association with the respective mRNA.

I also found that Kv1.2 and Kv3.4 channels showed no changes in protein expression in *Fmr1* KO mice in the brain areas studied for Kv4.2. Kv1.2 and Kv3.4 are key determinants of neuronal excitability. As previously stated, synaptic activity acutely regulates the channels that are critical determinants of dendritic excitability. This suggests that the exaggerated mGluR signaling seen in FXS may affect many Kv channels that are determinants of dendritic excitability, such as Kv1.2 and Kv3.4. However my data suggest that Kv1.2 and Kv3.4 mRNAs are not targets of FMRP, as their protein expression is not significantly altered in the absence of FMRP. A lack of dysregulated protein expression does not definitively determine that there is no association between these mRNAs and FMRP. More definitive evidence of binding

would be the analysis of FMRP-specific co-immunoprecipitates with Kv1.2 and Kv3.4 specific primers.

Data from Chen et al. demonstrating that the deletion of the Kv4.2 gene in mice eliminates the dendritic A-type currents in hippocampal CA1 neurons and Singh et al. demonstrating that a mutation in Kv4.2 has been linked to TLE promote the putative role of Kv4.2 as an important molecular determinant of FXS-related epilepsy (Chen et al., 2006; Singh et al., 2006). Future experiments to corroborate the importance of Kv4.2 in FXS-hyperexcitability could involve electrophysiological studies on either cultured *Fmr1* KO neurons or on brain slices. We would expect to observe altered A-type currents as a consequence of the downregulation of Kv4.2 protein.

Kv4.2 mRNA may localize in hippocampal dendrites

My data suggests that may Kv4.2 mRNA localize in the dendrites of the CA1 and the dentate gyrus. High background staining made absolute identification of Kv4.2 mRNA difficult, but the data still suggests that translation of Kv4.2 may occur locally in those regions. Raab-Graham et al. demonstrated that the potassium channel Kv1.1 is translated locally in the same regions (Raab-Graham et al., 2006). The localization and translation of Kv1.1 mRNA in dendrites implies regulation by an mRNA binding protein. A potential candidate is FMRP. In the future it would be interesting to determine whether Kv1.1 mRNA associates with FMRP as well and is translationally dysregulated in the absence of FMRP. Local dendritic translation has broad implications for the role of dendrites in synaptic plasticity. The dendritic localization of Kv4.2 mRNA in conjunction with the observed association of FMRP with Kv4.2 mRNA might play an important role for the mechanisms underlying FMRP-dependent regulation of dendritic Kv4.2 protein

expression. In a comment on Raab-Graham's study, Clark et al. posit that this work greatly expands the potential mechanisms whereby synaptic activity acutely regulates the Kv channels that are critical determinants of dendritic excitability (Clark et al., 2006).

In future experiments, it would be interesting to study potential local dendritic translation of Kv4.2 by using techniques outlined in this study (Raab-Graham et al., 2006). If Kv4.2 mRNA is later definitively confirmed to localize in hippocampal dendrites of the CA1 and dentate gyrus, then the next step would be to visualize and quantify local translation rates within lives cells. Raab-Graham et al. used a recombinant photoconvertible protein to allow for the live cell imaging of Kv1.1 translation. A photoconvertible protein is a fluorescent protein that, when hit with a certain wavelength, changes its fluorescent emission (Shaner et al., 2007). Raab-Graham et al. fused Kaede, a photoconvertible protein, to the 3' UTR of Kv1.1. When exposed to UV light Kaede is cleaved, changing its fluorescent emission from green to red. Raab-Graham et al. used this method to distinguish newly synthesized Kv1.1protein from pre-existing molecules in the dendrites of live neuronal cultures. The observed rapid occurrence of newly synthesized Kv1.1 in dendrites suggested that the protein was locally translated and not synthesized in the soma and shuttled into dendrites. We expect that this method would be suitable to test our hypothesis of local Kv4.2 translation in hippocampal dendrites.

Raab-Graham et al. also report that both endogenous Kv1.1 mRNA and newly synthesized Kv1.1 protein were found prominently in dendrites associated with translational "hotspots". Translational "hotspots" are regions near the synapse where protein synthesis occurs consistently over time. Aakalu et al. demonstrated that certain areas of dendrites show greater translation (17-fold increase) than other areas (Aakalu et

al., 2001). They termed these areas of increased dendritic translation "hotspots". We would expect that Kv4.2 protein will show similar localization.

Besides a potential role of FMRP in translational activation of Kv4.2 mRNA, a function in stabilizing Kv4.2 mRNA could also account for the reduced Kv4.2 protein levels observed in the absence of FMRP. A recent study suggested that FMRP positively regulates the mRNA stability of PSD95 (Zalfa et al., 2007). In this study RNA was isolated at 2 hour increments after application of the transcriptional inhibitor actinomycin D to cultured hippocampal neurons from both wild type and *Fmr1* KO mice, and decay rates of PSD95 mRNA were determined using quantitative real time PCR. In future studies, a similar experiment for Kv4.2 mRNA would determine if FMRP controls the stability of Kv4.2 mRNA.

Remarkably, Zalfa et al. also found that stabilization of PSD95 mRNA was dependent on brain areas, with the stabilization effect most prominently occurring in the hippocampus. Based on their observations, they suggest that FMRP regulates target mRNAs differently depending on the brain area (hippocampus or cortex). This supports our hypothesis to explain why western blot analyses of cortical and hippocampal brain lysates and synaptic compartments did not reflect the differences in Kv4.2 protein expression observed in immunostainings of hippocampal dendritic areas. We posit that this is due to different brain areas and cell compartments that were analyzed (page 24).

Summary

The goal of my thesis was to elucidate the underlying mechanisms for the high occurrence of epilepsy in fragile X patients. My study focused on one particular voltage-gated ion channel, Kv4.2, whose dysregulation is known to be involved in human

temporal lobe epilepsy. Using a mouse model, I used immunohistochemistry to demonstrate that Kv4.2 is reduced in the *FMR1* knockout mouse. Similar studies on other ion channels and receptors suggest that the downregulation in the knockout is specific to Kv4.2. My biochemical studies suggest that changes in Kv4.2 protein expression in the knockout may also be brain-region and cell-compartment specific. Together, these data support our hypothesis that Kv4.2 may be an important molecular determinant of FXS-related epilepsy. In future studies, we hope that further exploring the binding interactions of FMRP and Kv4.2 mRNA will help lead to a therapeutic solution to FXS-related epilepsy.

REFERENCES

Aakalu, G., Smith, W.B., Nguyen, N., Jiang, C., and Schuman, E.M. (2001). Dynamic visualization of local protein synthesis in hippocampal neurons. Neuron *30*, 489-502.
Bassell, G.J., and Warren, S.T. (2008). Fragile X syndrome: loss of local mRNA regulation alters synaptic development and function. Neuron *60*, 201-214.
Bear, M.F., Huber, K.M., and Warren, S.T. (2004). The mGluR theory of fragile X mental retardation. Trends Neurosci *27*, 370-377.
Bechara, E.G., Didiot, M.C., Melko, M., Davidovic, L., Bensaid, M., Martin, P., Castets, M., Pognonec, P., Khandjian, E.W., Moine, H., and Bardoni, B. (2009). A novel function for fragile X mental retardation protein in translational activation. PLoS Biol *7*, e16.
Beckett, L., Yu, Q., and Long, A.N. (2005). The Impact of Fragile X: Prevalence, Numbers Affected, and Economic Impact. The National Fragile X Foundation Quarterly, 18-21.
Berry-Kravis, E. (2002). Epilepsy in fragile X syndrome. Dev Med Child Neurol *44*, 724-728.
Birnbaum, S.G., Varga, A.W., Yuan, L.L., Anderson, A.E., Sweatt, J.D., and Schrader, L.A. (2004). Structure and function of Kv4-family transient potassium channels. Physiol Rev *84*, 803-833.
Bobrow, M.N., and Moen, P.T., Jr. (2001). Tyramide signal amplification (TSA) systems for the enhancement of ISH signals in cytogenetics. Curr Protoc Cytom *Chapter 8*, Unit 8 9.
Chen, X., Yuan, L.L., Zhao, C., Birnbaum, S.G., Frick, A., Jung, W.E., Schwarz, T.L., Sweatt, J.D., and Johnston, D. (2006). Deletion of Kv4.2 gene eliminates dendritic A-type K+ current and enhances induction of long-term potentiation in hippocampal CA1 pyramidal neurons. J Neurosci *26*, 12143-12151.
Cho, S., Park, S.M., Kim, T.D., Kim, J.H., Kim, K.-T., and Jang, S.K. (2007). BiP Internal Ribosomal Entry Site Activity Is Controlled by Heat-Induced Interaction of NSAP1. Mol. Cell. Biol. *27*, 368-383.
Chuang, S.C., Zhao, W., Bauchwitz, R., Yan, Q., Bianchi, R., and Wong, R.K. (2005). Prolonged epileptiform discharges induced by altered group I metabotropic glutamate receptor-mediated synaptic responses in hippocampal slices of a fragile X mouse model. J Neurosci *25*, 8048-8055.
Clark, E., Vacher, H., and Trimmer, J.S. (2006). Kv1.1 takes a deTOR from the axon to the dendrite. Neuron *52*, 399-401.
Comery, T.A., Harris, J.B., Willems, P.J., Oostra, B.A., Irwin, S.A., Weiler, I.J., and Greenough, W.T. (1997). Abnormal dendritic spines in fragile X knockout mice: maturation and pruning deficits. PNAS *94*, 5401-5404.
Darnell, J.C., Fraser, C.E., Mostovetsky, O., Stefani, G., Jones, T.A., Eddy, S.R., and Darnell, R.B. (2005). Kissing complex RNAs mediate interaction between the Fragile-X mental retardation protein KH2 domain and brain polyribosomes. Genes Dev.
Davidkova, G., and Carroll, R.C. (2007). Characterization of the Role of Microtubule-Associated Protein 1B in Metabotropic Glutamate Receptor-Mediated Endocytosis of AMPA Receptors in Hippocampus. J. Neurosci. *27*, 13273-13278.

Dictenberg, J.B., Swanger, S.A., Antar, L.N., Singer, R.H., and Bassell, G.J. (2008). A direct role for FMRP in activity-dependent dendritic mRNA transport links filopodial-spine morphogenesis to fragile X syndrome. Dev Cell *14*, 926-939.
Dolen, G., Osterweil, E., Rao, B.S., Smith, G.B., Auerbach, B.D., Chattarji, S., and Bear, M.F. (2007). Correction of fragile X syndrome in mice. Neuron *56*, 955-962.
Eberhart, D.E., Malter, H.E., Feng, Y., and Warren, S.T. (1996). The fragile X mental retardation protein is a ribonucleoprotein containing both nuclear localization and nuclear export signals. Hum Mol Genet *5*, 1083-1091.
Feng, Y., Absher, D., Eberhart, D.E., Brown, V., Malter, H.E., and Warren, S.T. (1997a). FMRP associates with polyribosomes as an mRNP, and the I304N mutation of severe fragile X syndrome abolishes this association. Mol Cell *1*, 109-118.
Feng, Y., Gutekunst, C.A., Eberhart, D.E., Yi, H., Warren, S.T., and Hersch, S.M. (1997b). Fragile X mental retardation protein: nucleocytoplasmic shuttling and association with somatodendritic ribosomes. J Neurosci *17*, 1539-1547.
Fisch, G.S., Simensen, R.J., and Schroer, R.J. (2002). Longitudinal changes in cognitive and adaptive behavior scores in children and adolescents with the fragile X mutation or autism. J Autism Dev Disord *32*, 107-114.
Fu, Y.H., Kuhl, D.P., Pizzuti, A., Pieretti, M., Sutcliffe, J.S., Richards, S., Verkerk, A.J., Holden, J.J., Fenwick, R.G., Jr., Warren, S.T., and et al. (1991). Variation of the CGG repeat at the fragile X site results in genetic instability: resolution of the Sherman paradox. Cell *67*, 1047-1058.
Gross, C., and Bassell, G.J. (2008). Cutting down on glutamate signaling pays off for fragile x syndrome. Nature Medicine *in press*.
Grossman, A.W., Aldridge, G.M., Weiler, I.J., and Greenough, W.T. (2006). Local protein synthesis and spine morphogenesis: Fragile X syndrome and beyond. J Neurosci *26*, 7151-7155.
Hagerman, P.J., Greco, C.M., and Hagerman, R.J. (2003). A cerebellar tremor/ataxia syndrome among fragile X premutation carriers. Cytogenet Genome Res *100*, 206-212.
Hagerman, R.J., Hull, C.E., Safanda, J.F., Carpenter, I., Staley, L.W., O'Connor, R.A., Seydel, C., Mazzocco, M.M., Snow, K., Thibodeau, S.N., and et al. (1994). High functioning fragile X males: demonstration of an unmethylated fully expanded FMR-1 mutation associated with protein expression. Am J Med Genet *51*, 298-308.
Harrison, C.J., Jack, E.M., Allen, T.D., and Harris, R. (1983). The fragile X: a scanning electron microscope study. J Med Genet *20*, 280-285.
Hou, L., Antion, M.D., Hu, D., Spencer, C.M., Paylor, R., and Klann, E. (2006). Dynamic translational and proteasomal regulation of fragile X mental retardation protein controls mGluR-dependent long-term depression. Neuron *51*, 441-454.
Hu, H.J., Alter, B.J., Carrasquillo, Y., Qiu, C.S., and Gereau, R.W.t. (2007). Metabotropic glutamate receptor 5 modulates nociceptive plasticity via extracellular signal-regulated kinase-Kv4.2 signaling in spinal cord dorsal horn neurons. J Neurosci *27*, 13181-13191.
Huber, K.M., Gallagher, S.M., Warren, S.T., and Bear, M.F. (2002). Altered synaptic plasticity in a mouse model of fragile x mental retardation. PNAS *99*, 7746-7750.
Huttelmaier, S., Zenklusen, D., Lederer, M., Dictenberg, J., Lorenz, M., Meng, X., Bassell, G.J., Condeelis, J., and Singer, R.H. (2005). Spatial regulation of beta-actin translation by Src-dependent phosphorylation of ZBP1. Nature *438*, 512-515.

Irwin, S.A., Galvez, R., and Greenough, W.T. (2000). Dendritic spine structural anomalies in Fragile X Mental Retardation Syndrome. Cerebral Cortex *10*, 1038-1044.
Link, W., Konietzko, U., Kauselmann, G., Krug, M., Schwanke, B., Frey, U., and Kuhl, D. (1995). Somatodendritic expression of an immediate early gene is regulated by synaptic activity. PNAS *92*, 5734-5738.
Lu, R., Wang, H., Liang, Z., Ku, L., O'Donnell W, T., Li, W., Warren, S.T., and Feng, Y. (2004). The fragile X protein controls microtubule-associated protein 1B translation and microtubule stability in brain neuron development. Proc Natl Acad Sci U S A *101*, 15201-15206.
Lyford, G.L., Yamagata, K., Kaufman, W.E., Barnes, C.A., Sanders, L.K., Copeland, N.G., Gilbert, D.J., Jenkins, N.A., Lanahan, A.A., and Worley, P.F. (1995). ArC, a growth factor and activity related gene encodes a novel cytoskeletal protein that is enriched in neuronal dendrites. Neuron *14*, 433-445.
McBride, S.M., Choi, C.H., Wang, Y., Liebelt, D., Braunstein, E., Ferreiro, D., Sehgal, A., Siwicki, K.K., Dockendorff, T.C., Nguyen, H.T., *et al.* (2005). Pharmacological rescue of synaptic plasticity, courtship behavior, and mushroom body defects in a Drosophila model of fragile X syndrome. Neuron *45*, 753-764.
Menon, L., Mader, S.A., and Mihailescu, M.R. (2008). Fragile X mental retardation protein interactions with the microtubule associated protein 1B RNA. RNA *14*, 1644-1655.
Merlin, L.R., Bergold, P.J., and Wong, R.K. (1998). Requirement of protein synthesis for group I mGluR-mediated induction of epileptiform discharges. J Neurophysiol *80*, 989-993.
Muddashetty, R.S., Kelic, S., Gross, C., Xu, M., and Bassell, G.J. (2007). Dysregulated metabotropic glutamate receptor-dependent translation of AMPA receptor and postsynaptic density-95 mRNAs at synapses in a mouse model of fragile X syndrome. J Neurosci *27*, 5338-5348.
Musumeci, S.A., Hagerman, R.J., Ferri, R., Bosco, P., Dalla Bernardina, B., Tassinari, C.A., De Sarro, G.B., and Elia, M. (1999). Epilepsy and EEG findings in males with fragile X syndrome. Epilepsia *40*, 1092-1099.
Napoli, I., Mercaldo, V., Boyl, P.P., Eleuteri, B., Zalfa, F., De Rubeis, S., Di Marino, D., Mohr, E., Massimi, M., Falconi, M., *et al.* (2008). The fragile X syndrome protein represses activity-dependent translation through CYFIP1, a new 4E-BP. Cell *134*, 1042-1054.
Narayanan, U., Nalavadi, V., Nakamoto, M., Pallas, D.C., Ceman, S., Bassell, G.J., and Warren, S.T. (2007). FMRP phosphorylation reveals an immediate-early signaling pathway triggered by group I mGluR and mediated by PP2A. J Neurosci *27*, 14349-14357.
Narayanan, U., Nalavadi, V., Nakamoto, M., Thomas, G., Ceman, S., Bassell, G.J., and Warren, S.T. (2008). S6K1 phosphorylates and regulates fragile X mental retardation protein (FMRP) with the neuronal protein synthesis-dependent mammalian target of rapamycin (mTOR) signaling cascade. J Biol Chem *283*, 18478-18482.
Nosyreva, E.D., and Huber, K.M. (2006). Metabotropic receptor-dependent long-term depression persists in the absence of protein synthesis in the mouse model of fragile X syndrome. J Neurophysiol *95*, 3291-3295.

Oostra, B.A., and Willemsen, R. (2009). FMR1: A gene with three faces. Biochim Biophys Acta.
Park, S., Park, J.M., Kim, S., Kim, J.A., Shepherd, J.D., Smith-Hicks, C.L., Chowdhury, S., Kaufmann, W., Kuhl, D., Ryazanov, A.G., *et al.* (2008). Elongation factor 2 and fragile X mental retardation protein control the dynamic translation of Arc/Arg3.1 essential for mGluR-LTD. Neuron *59*, 70-83.
Penagarikano, O., Mulle, J.G., and Warren, S.T. (2007). The pathophysiology of fragile x syndrome. Annu Rev Genomics Hum Genet *8*, 109-129.
Price, T.J., Rashid, M.H., Millecamps, M., Sanoja, R., Entrena, J.M., and Cervero, F. (2007). Decreased nociceptive sensitization in mice lacking the fragile X mental retardation protein: role of mGluR1/5 and mTOR. J Neurosci *27*, 13958-13967.
Raab-Graham, K.F., Haddick, P.C., Jan, Y.N., and Jan, L.Y. (2006). Activity- and mTOR-dependent suppression of Kv1.1 channel mRNA translation in dendrites. Science *314*, 144-148.
Ronesi, J.A., and Huber, K.M. (2008). Homer interactions are necessary for metabotropic glutamate receptor-induced long-term depression and translational activation. J Neurosci *28*, 543-547.
Rousseau, F., Rouillard, P., Morel, M.L., Khandjian, E.W., and Morgan, K. (1995). Prevalence of carriers of premutation-size alleles of the FMRI gene--and implications for the population genetics of the fragile X syndrome. Am J Hum Genet *57*, 1006-1018.
Sambrook, J., Russell, D.W., and Cold Spring Harbor Laboratory. (2001). Molecular cloning : a laboratory manual, 3rd. edn (Cold Spring Harbor, N.Y.: Cold Spring Harbor Laboratory).
Shaner, N.C., Patterson, G.H., and Davidson, M.W. (2007). Advances in fluorescent protein technology. J Cell Sci *120*, 4247-4260.
Sherman, S.L., Jacobs, P.A., Morton, N.E., Froster-Iskenius, U., Howard-Peebles, P.N., Nielsen, K.B., Partington, M.W., Sutherland, G.R., Turner, G., and Watson, M. (1985). Further segregation analysis of the fragile X syndrome with special reference to transmitting males. Hum Genet *69*, 289-299.
Sherman, S.L., Morton, N.E., Jacobs, P.A., and Turner, G. (1984). The marker (X) syndrome: a cytogenetic and genetic analysis. Ann Hum Genet *48*, 21-37.
Singh, B., Ogiwara, I., Kaneda, M., Tokonami, N., Mazaki, E., Baba, K., Matsuda, K., Inoue, Y., and Yamakawa, K. (2006). A Kv4.2 truncation mutation in a patient with temporal lobe epilepsy. Neurobiology of Disease *24*, 245-253.
Teleman, A.A., Chen, Y.W., and Cohen, S.M. (2005). 4E-BP functions as a metabolic brake used under stress conditions but not during normal growth. Genes Dev *19*, 1844-1848.
Tiedge, H., Fremeau, J., R T, Weinstock, P.H., and Arancio, O. (1991). Dendritic location of neural BC1 RNA. Pro. Natl. Acad. Sci. USA *88*, 2093-2097.
Todd, P.K., Mack, K.J., and Malter, J.S. (2003). The fragile X mental retardation protein is required for type-I metabotropic glutamate receptor-dependent translation of PSD-95. Proc Natl Acad Sci U S A *100*, 14374-14378.
Tucker, B., Richards, R.I., and Lardelli, M. (2006). Contribution of mGluR and Fmr1 functional pathways to neurite morphogenesis, craniofacial development and fragile X syndrome. Hum Mol Genet *15*, 3446-3458.

Verkerk, A.J., Pieretti, M., Sutcliffe, J.S., Fu, Y.H., Kuhl, D.P., Pizzuti, A., Reiner, O., Richards, S., Victoria, M.F., Zhang, F.P., *et al.* (1991). Identification of a gene (FMR-1) containing a CGG repeat coincident with a breakpoint cluster region exhibiting length variation in fragile X syndrome. Cell *65*, 905-914.
Waung, M.W., Pfeiffer, B.E., Nosyreva, E.D., Ronesi, J.A., and Huber, K.M. (2008). Rapid translation of Arc/Arg3.1 selectively mediates mGluR-dependent LTD through persistent increases in AMPAR endocytosis rate. Neuron *59*, 84-97.
Weiler, I.J., Spangler, C.C., Klintsova, A.Y., Grossman, A.W., Kim, S.H., Bertaina-Anglade, V., Khaliq, H., de Vries, F.E., Lambers, F.A., Hatia, F., *et al.* (2004). Fragile X mental retardation protein is necessary for neurotransmitter-activated protein translation at synapses. Proc Natl Acad Sci U S A *101*, 17504-17509.
Westmark, C.J., and Malter, J.S. (2007). FMRP Mediates mGluR5-Dependent Translation of Amyloid Precursor Protein. PLoS Biology *5*, e52.
Yan, Q.J., Rammal, M., Tranfaglia, M., and Bauchwitz, R.P. (2005). Suppression of two major Fragile X Syndrome mouse model phenotypes by the mGluR5 antagonist MPEP. Neuropharmacology *49*, 1053-1066.
Zalfa, F., Adinolfi, S., Napoli, I., Kuhn-Holsken, E., Urlaub, H., Achsel, T., Pastore, A., and Bagni, C. (2005). FMRP binds specifically to the brain cytoplasmic RNAs BC1/BC200 via a novel RNA binding motif. J Biol Chem.
Zalfa, F., Eleuteri, B., Dickson, K.S., Mercaldo, V., De Rubeis, S., di Penta, A., Tabolacci, E., Chiurazzi, P., Neri, G., Grant, S.G., and Bagni, C. (2007). A new function for the fragile X mental retardation protein in regulation of PSD-95 mRNA stability. Nat Neurosci *10*, 578-587.
Zalfa, F., Giorgi, M., Primerano, B., Moro, A., Di Penta, A., Reis, S., Oostra, B., and Bagni, C. (2003). The fragile X syndrome protein FMRP associates with BC1 RNA and regulates the translation of specific mRNAs at synapses. Cell *112*, 317-327.
Zhang, Y.Q., Bailey, A.M., Matthies, H.J., Renden, R.B., Smith, M.A., Speese, S.D., Rubin, G.M., and Broadie, K. (2001). Drosophila Fragile X-related gene regulates the MAP1b homolog Futsch to control synaptic structure and function. Cell *107*, 591-603.

FIGURES

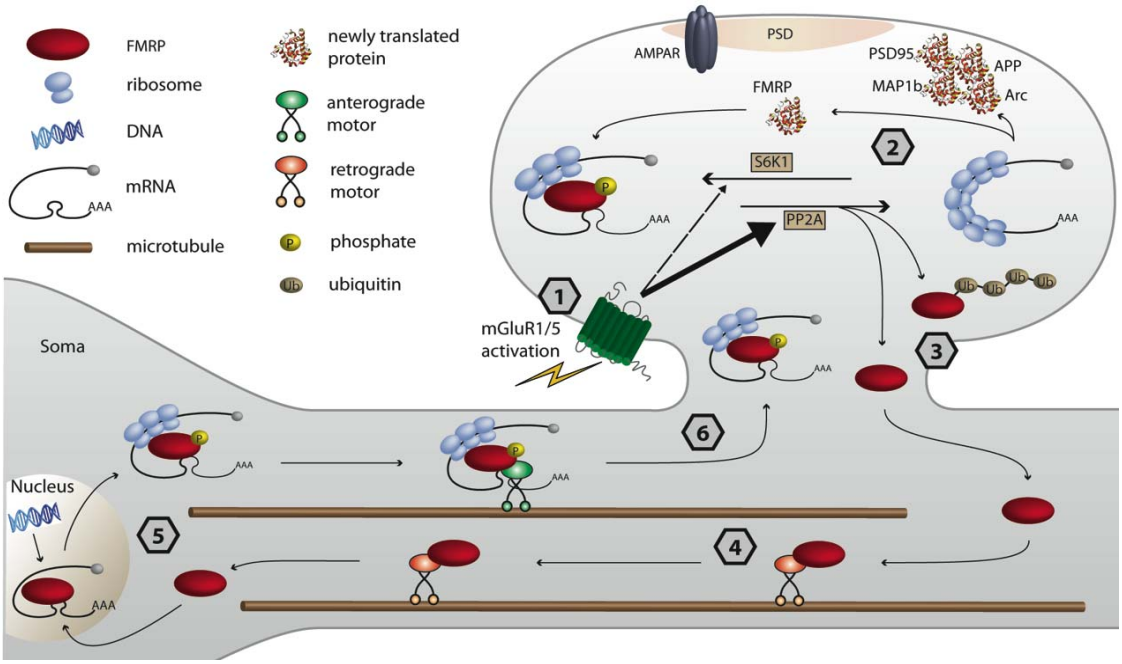

Figure 1. Proposed functions of FMRP throughout the neuron. This figure shows the role of FMRP for mGluR-mediated translational derepression of mRNAs (1-3) and activity-induced dendritic mRNA transport (4-6). Newly synthesized proteins include for example proteins that regulate AMPA receptor endocytosis at synapses (Davidkova and Carroll, 2007; Hou et al., 2006; Muddashetty et al., 2007; Park et al., 2008; Todd et al., 2003; Waung et al., 2008; Westmark and Malter, 2007). Derepression of translation might be regulated by gp1 mGluR-induced dephosphorylation (2) (Narayanan et al., 2007; Narayanan et al., 2008) and by ubiquitination, followed by proteasomal degradation (3) (Hou et al., 2006). (4-6) Apart from translation, FMRP also regulates mRNA transport. FMRP can shuttle between the nucleus and cytoplasm (Eberhart et al., 1996; Feng et al., 1997b) and was shown to be involved in activity induced bidirectional dendritic transport of target mRNA (Dictenberg et al., 2008) . Reprinted from Neuron, Volume 60, Issue 2, (Bassell and Warren, 2008), Fragile X Syndrome: Loss of Local mRNA Regulation Alters Synaptic Development and Function, Page 210, Copyright (2008), with permission from Elsevier.

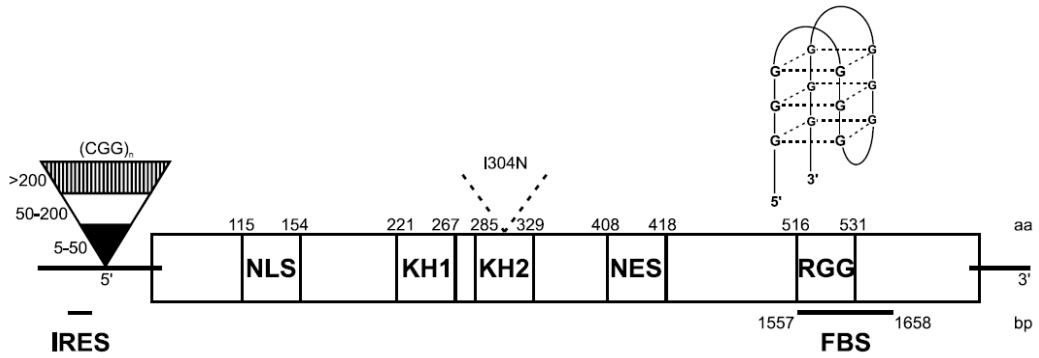

Figure 2. Protein domain structure of the mRNA binding protein fragile X mental retardation protein (FMRP). NLS, nuclear localization signal; KH1 and KH2, RNA-binding domains; NES, nuclear export signal; RGG, RGG box, RNA binding. FMRP is expressed from the *FMR1* gene. See introduction for details.

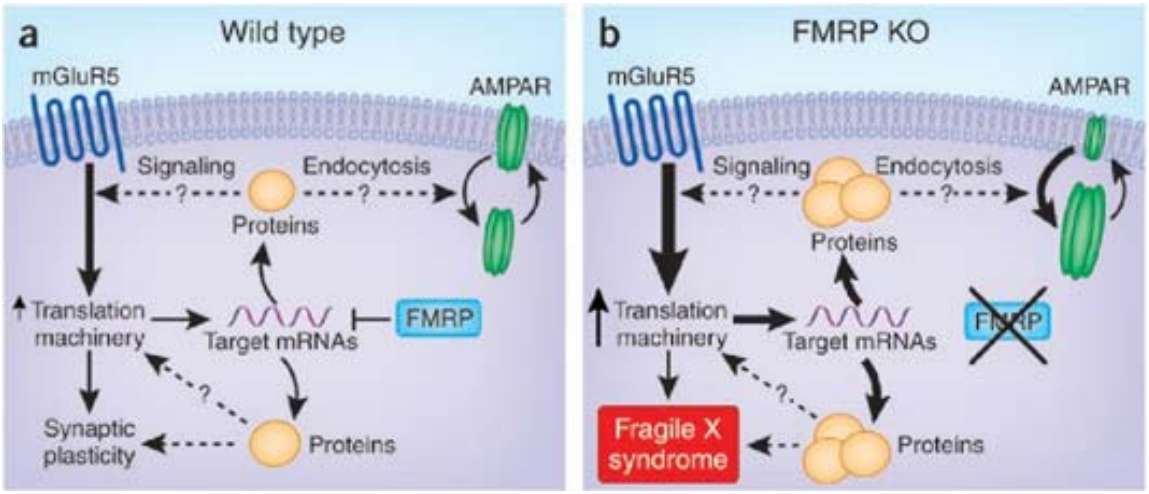

Figure 3. Model of mGluR theory. (a) mGluR5 signaling in wild type mice activates the translation machinery and induces specific protein synthesis–dependent forms of synaptic plasticity. Some of the mGluR5-regulated mRNAs are translationally suppressed by fragile X mental retardation protein (FMRP). (b) In *Fmr1* KO mice (FMRP KO), FMRP target mRNAs are translated excessively and mGluR5 signaling is exaggerated. Adapted by permission from Macmillan Publishers Ltd: [Nature Medicine]
(Gross and Bassell, 2008), copyright (2008)

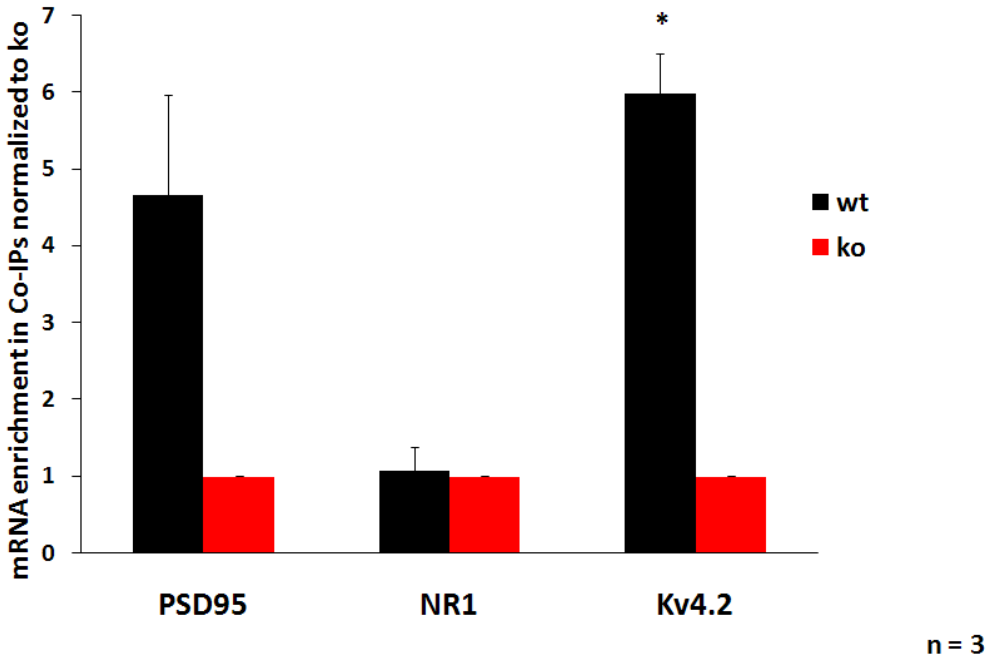

Figure 4. Kv4.2 mRNA is associated with FMRP in co-immunoprecipitation experiments using a specific FMRP antibody. Kv4.2 mRNA is significantly enriched in immunoprecipitates from wild type (WT) mouse tissue compared to *Fmr1* knockout (KO) mouse tissue. PSD95 is a validated target mRNA of FMRP and served as positive control. NR1 mRNA does not associate with FMRP, thus NR1 protein was used as a negative control in the immunostaining experiments. Figure provided by Christina Gross (Bassell lab– Unpublished).

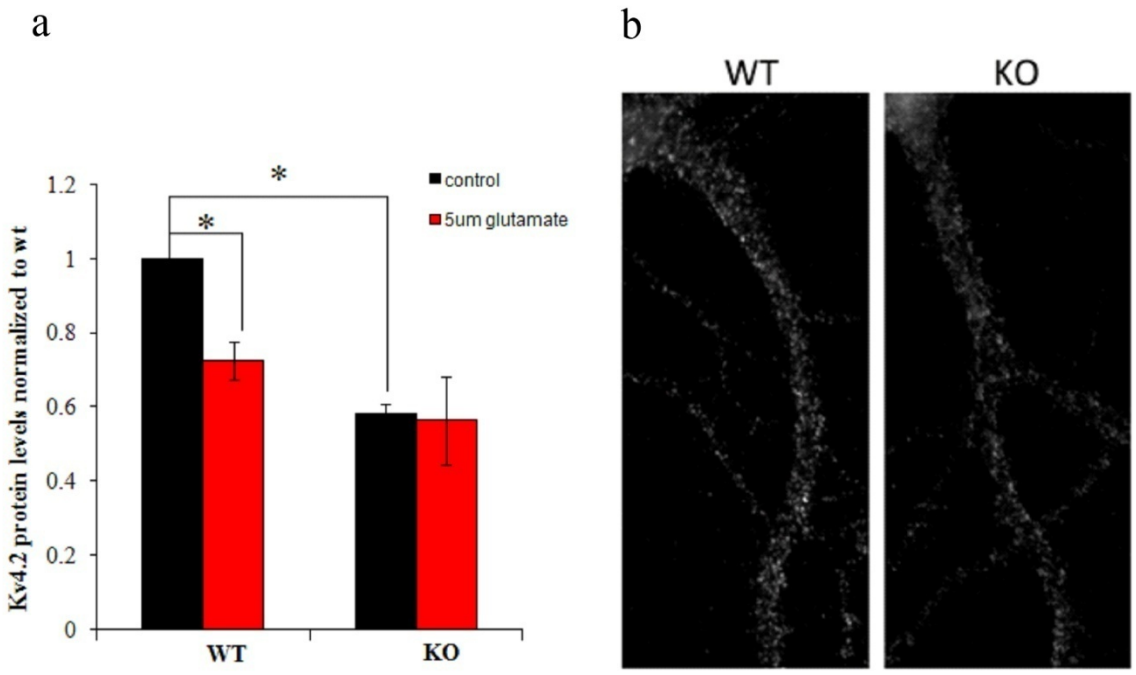

Figure 5. Glutamate induced reduction of Kv4.2 protein levels in dendrites is abolished in cultured *Fmr1* KO neurons. (A) Altered Kv4.2 protein expression in primary cultured *Fmr1* KO hippocampal neurons. Neurons were treated with or without 5μM glutamate for 10 minutes before fixation. Quantitative analysis of Kv4.2 immunostaining shows that Kv4.2 protein levels are about 40% lower in *Fmr1* KO dendrites at basal stage compared to WT. Glutamate stimulation induced a 30% decrease of Kv4.2 protein levels in WT dendrites as reported previously; however, this reduction was abolished in *Fmr1* KO (n=3, paired t-test *$p<0.05$). (B) Representative cultured hippocampal neuron immunostaining for Kv4.2. The KO shows weaker signal as compared to the WT. This result indicates that there is an impaired regulation of Kv4.2 protein in the absence of FMRP. Figure provided by Xiaodi Yao (Bassell lab – Unpublished).

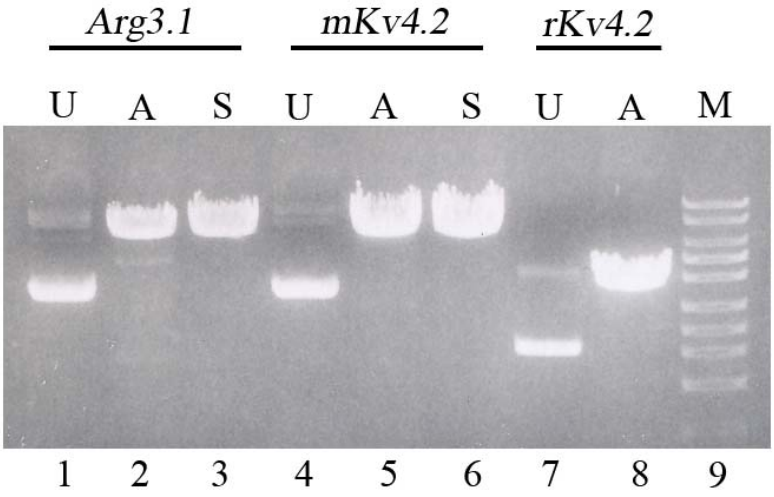

Figure 6. DNA restriction. Plasmids containing cDNAs for Arg3.1, mouse Kv4.2 (mKv4.2) and rat Kv4.2 (rKv4.2) DNA were linearized with different restriction enzymes to allow for in vitro transcription of antisense (A) and sense (S) constructs. Arg3.1 was used as a control in the *in situ* hybridization experiments. Uncut (U) plasmids were run on the same gel (lanes 1, 4, and 8). Uncut plasmids were still supercoiled and thus traveled further through the gel than the linearized plasmids (lanes 2, 3, 5, 6, and 8).

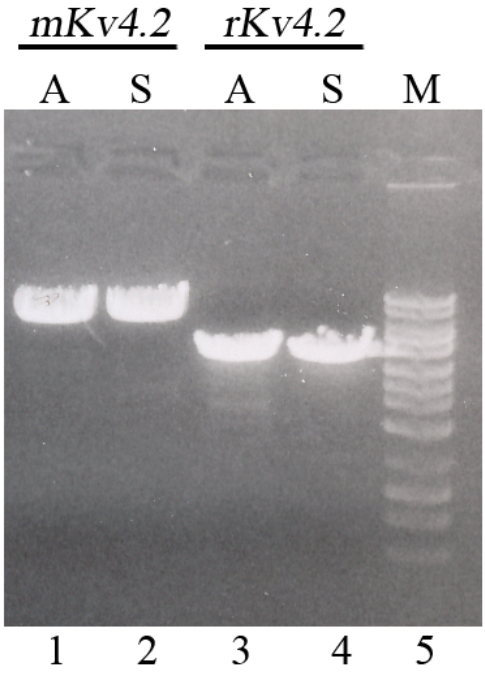

Figure 7. DNA analysis after phenol-chloroform extraction. Linearized plasmids containing cDNA constructs for the generation of antisense (A) and sense (S) mouse Kv4.2 (mKv4.2) and rat Kv4.2 (rKv4.2) riboprobes were purified by phenol-chloroform extraction. Phenol-chloroform extraction is a liquid-liquid extraction technique that was used to isolate DNA from the restriction enzymes used to linearize the plasmids containing the constructs. This gel shows that the DNA strands remain linearized, in comparison to the uncut plasmids (lanes 4, 7 in Figure 4).

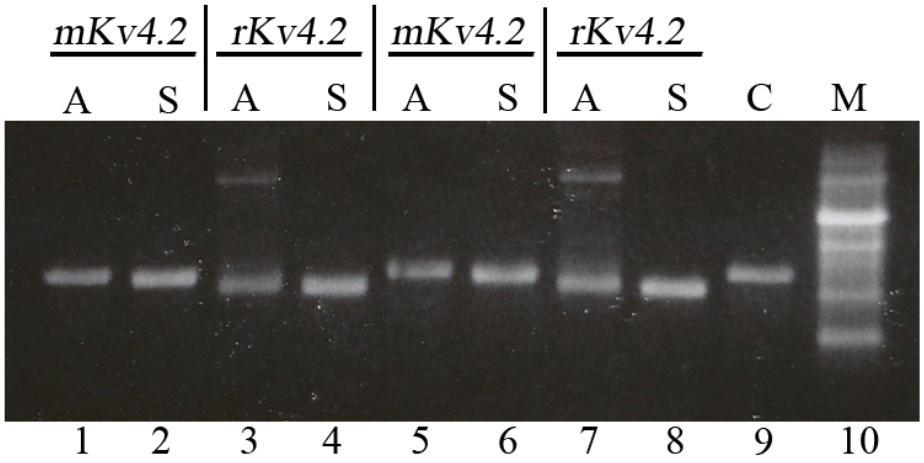

Figure 8. Results of *in vitro* transcription. Antisense (A) and sense (S) RNA strands (riboprobes) were generated for mouse Kv4.2 (mKv4.2) and rat Kv4.2 (rKv4.2) cDNA in an *in vitro* transcription experiment. Lanes 1-8 show RNA that was generated in the *in vitro* transcription while lane 9 (C) is control RNA.

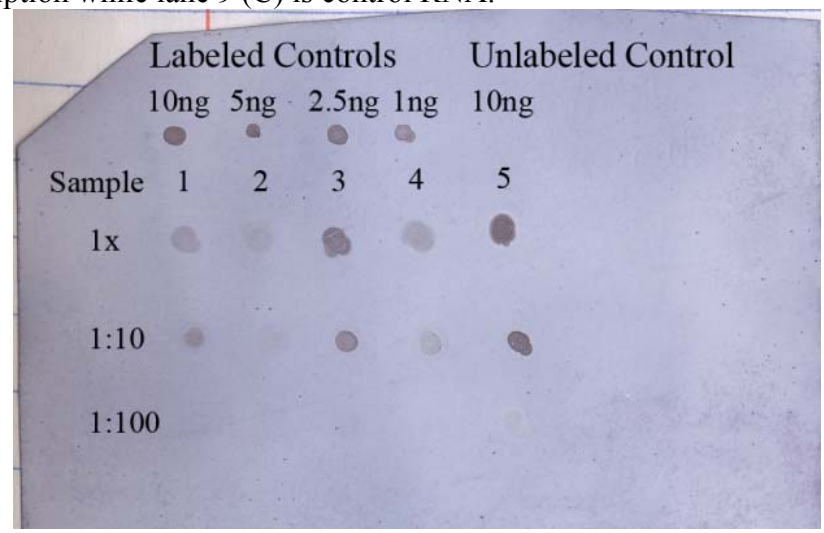

Figure 9. Incorporation of digoxigenin-labeled UTP into *in vitro* transcribed RNA. In order to detect the mRNA riboprobes, UTP nucleotides with Dioxigenin (DIG) tags are used in the *in vitro* transcription experiments. The DIG labels are detected using anti-DIG antibodies in the *in situ* hybridization experiments. This example dot blot confirms the incorporation of DIG labels into the RNA probes (riboprobes). Diluted riboprobe samples are compared to controls with known concentrations to estimate concentrations of riboprobes.

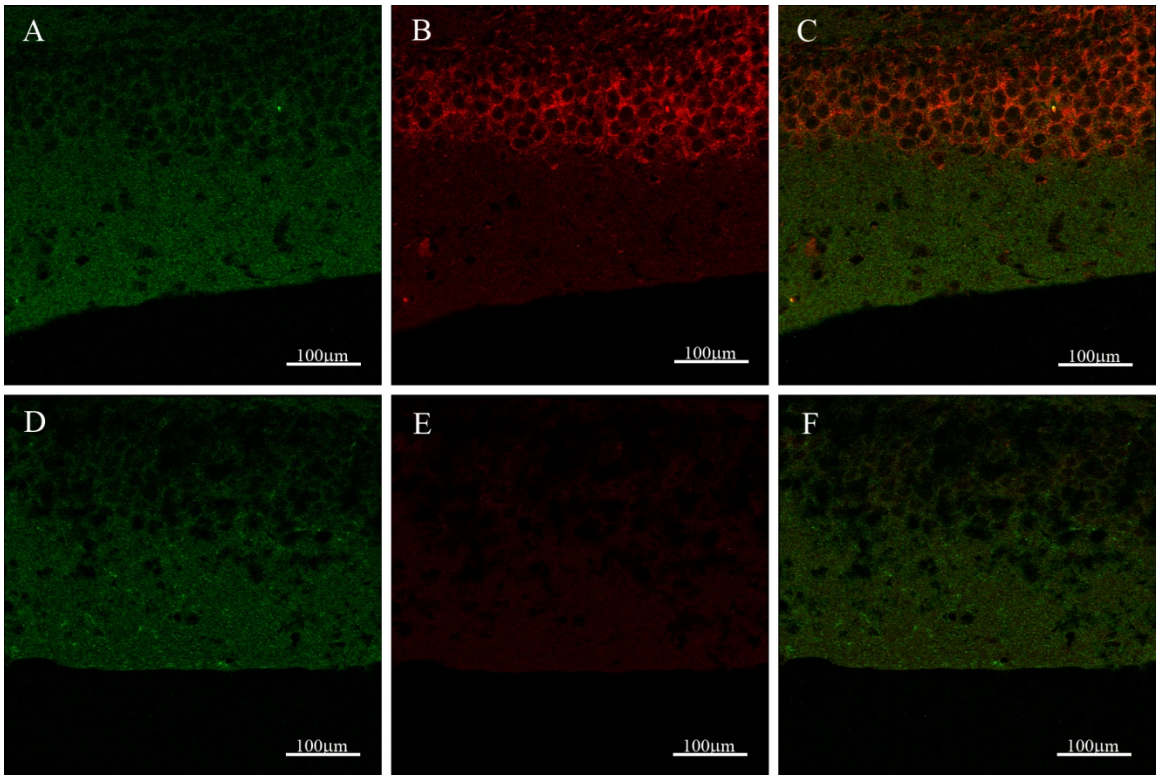

Figure 10. Representative immunostainings demonstrating the absence of FMRP in *Fmr1*- knockout mouse model. To ascertain that the *Fmr1* knockout (KO) mouse model was valid, I conducted immunostainings for Kv4.2 (green) and FMRP (red) on wild type and *Fmr1* KO mice. Images A-C represent a wild type dentate gyrus co-stained for Kv4.2 (A) and FMRP (B); the overlay is shown in C. Images D-F represent corresponding stainings in dentate gyrus from *Fmr1* KO mice. The WT and KO brain sections were immunostained on the same microscope slide. In the KO brain, there is no signal beyond background for FMRP.

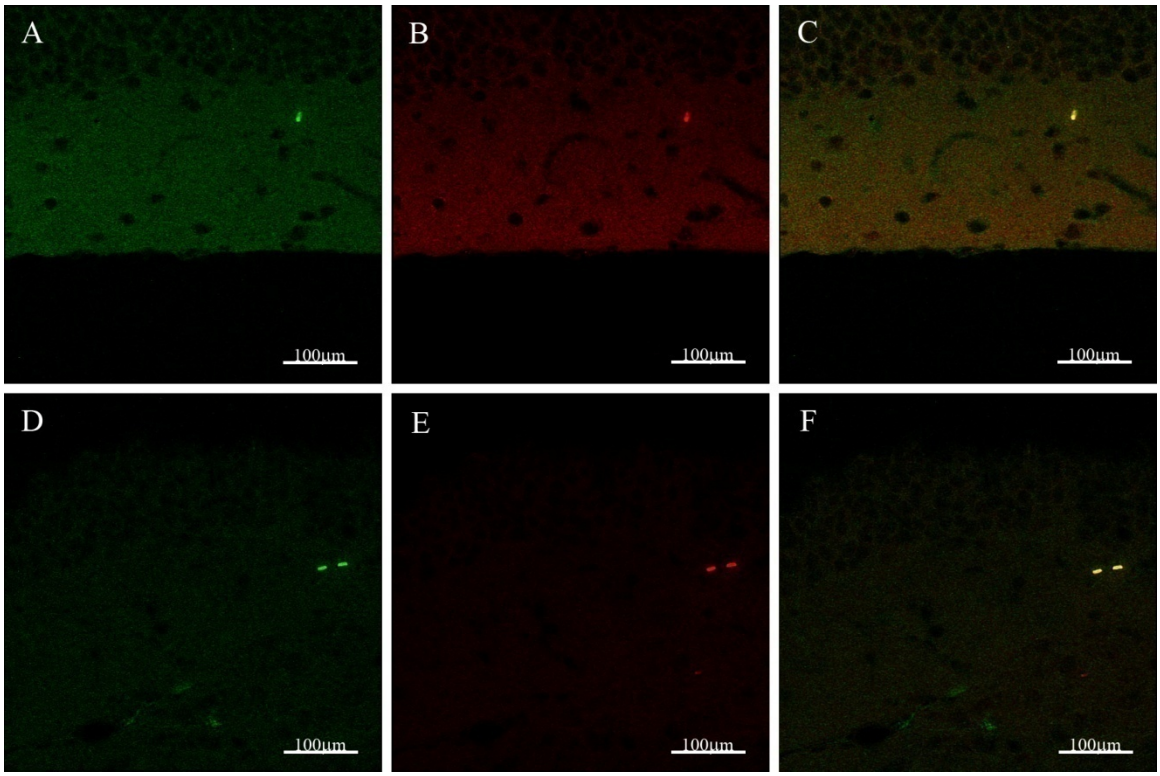

Figure 11. Representative background signal in immunostainings. Images A-C represent one *Fmr1*- knockout dentate gyrus stained for Kv1.2 (A, green) and Kv4.2 (B, red), and an overlay (C). Images D-F represent immunostainings of a brain slice from the same brain as A-C with the primary antibodies omitted. Image D shows Cy2 (green) background staining, image E shows Cy3 (red) background staining and image F shows the overlay of D and E. Quantification and subtraction of background signal did not alter the trends or significance of the immunostainings experiments (data not shown).

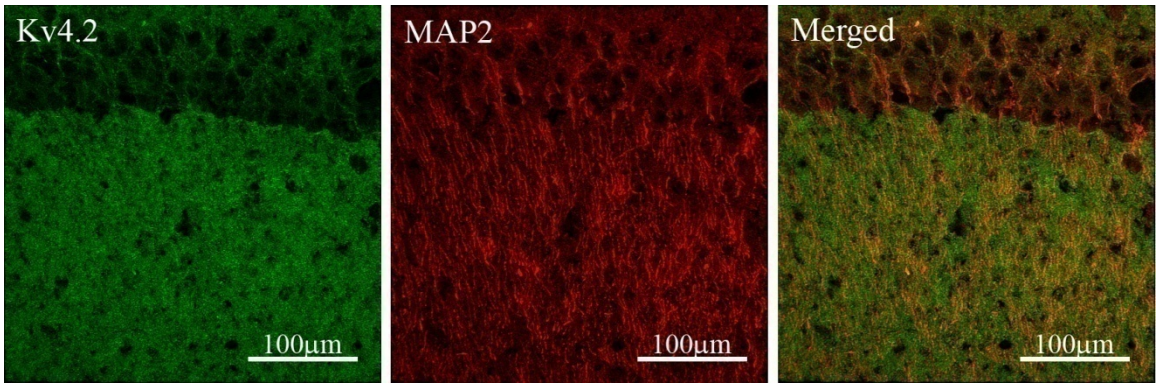

Figure 12. Representative immunostaining of Kv4.2 in hippocampal dendrites. Shown is a representative immunostaining of Kv4.2 (green) and MAP2 (red) in the CA1 region of the hippocampus along with an overlay image of the two signals. MAP2 is a neuron-specific cytoskeletal protein that is highly enriched in dendrites. Immunostaining using a rabbit MAP2 antibody highlights individual dendrites (middle box).

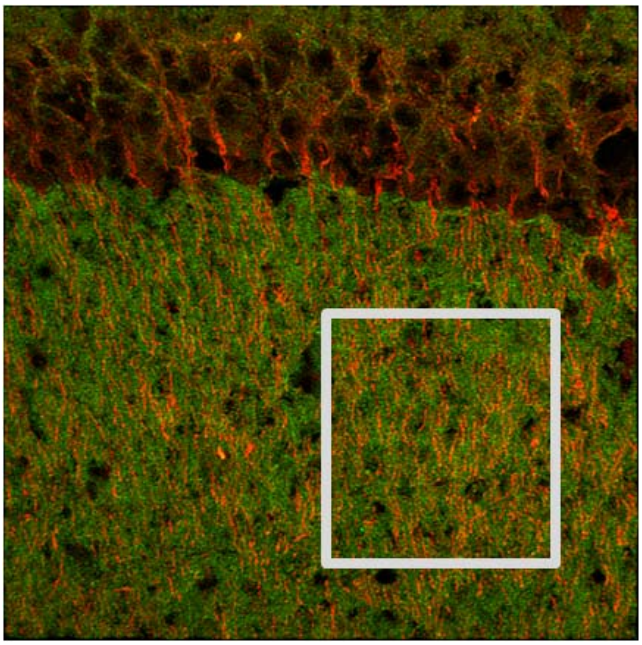

Figure 13. Example of the area of dendritic region quantified. This is a representative immunostaining of Kv4.2 (green) and MAP2 (red) in the CA1 region of the hippocampus. The white box indicates an area used for quantification. The cell body layer (at the top of the image) and areas with tears were not quantified.

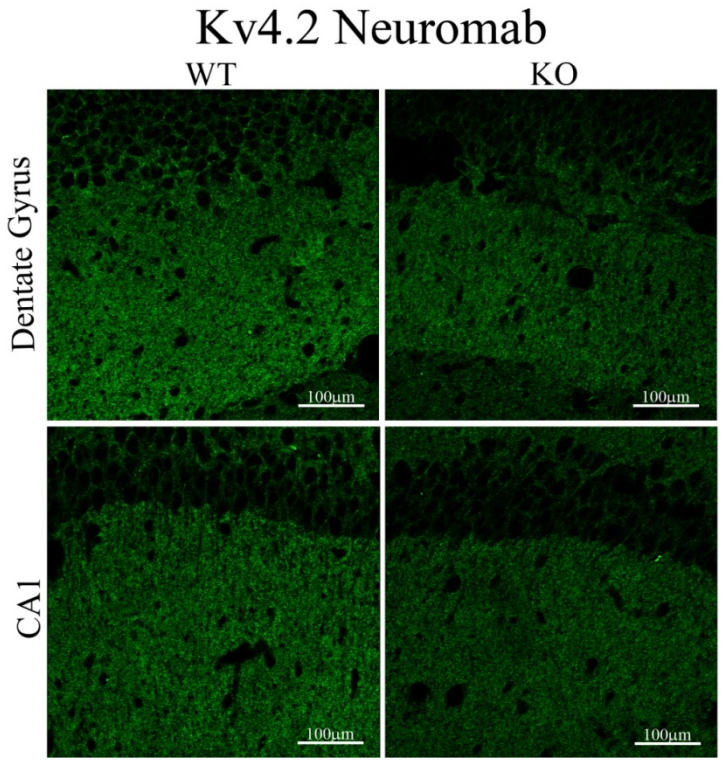

Figure 14. Kv4.2 protein is reduced in dendritic regions of the *Fmr1*-KO hippocampus. This is a representative immunostaining of quantitative analysis shown in Figure 15. I conducted fluorescence immunostainings using a specific, anti-mouse Kv4.2 antibody from Neuromab on hippocampal brain sections of wild type and *Fmr1* knockout (KO) in the dentate gyrus and CA1 regions.

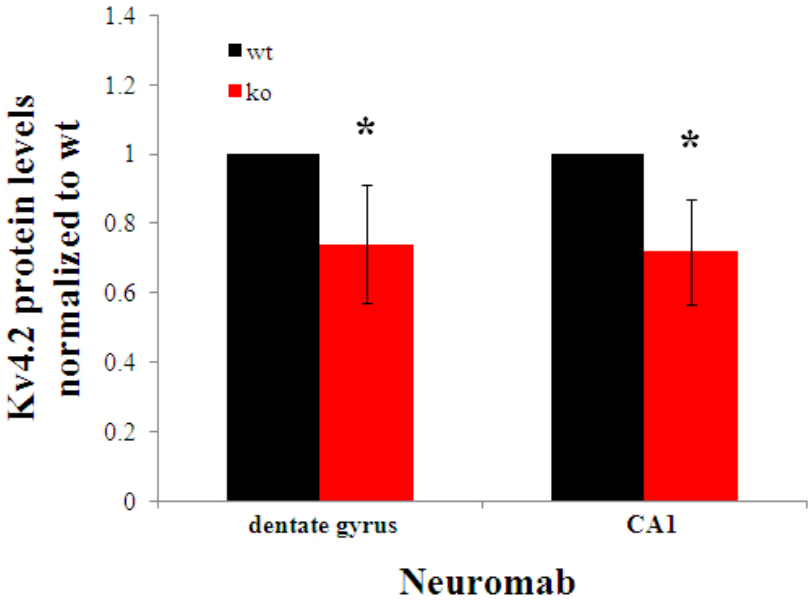

Figure 15. Kv4.2 protein is significantly reduced in hippocampal dendrites of *Fmr1* KO mice. Quantification of Kv4.2 protein in the dendrites of the dentate gyrus (DG) and CA1 region of the hippocampus showed significant downregulation of Kv4.2 protein in the *Fmr1* knockout (KO). KO signal intensities were normalized to the wild type (WT) in each experiment. Quantitative analysis of Kv4.2 immunostainings showed a significant 26% reduction of Kv4.2 protein in the KO DG (n=6, paired t-test, *p= 0.013). Similarly, quantitative analysis of Kv4.2 immunostainings in the CA1 region showed a significant 28% reduction (n=6, paired t-test, *p= 0.006).

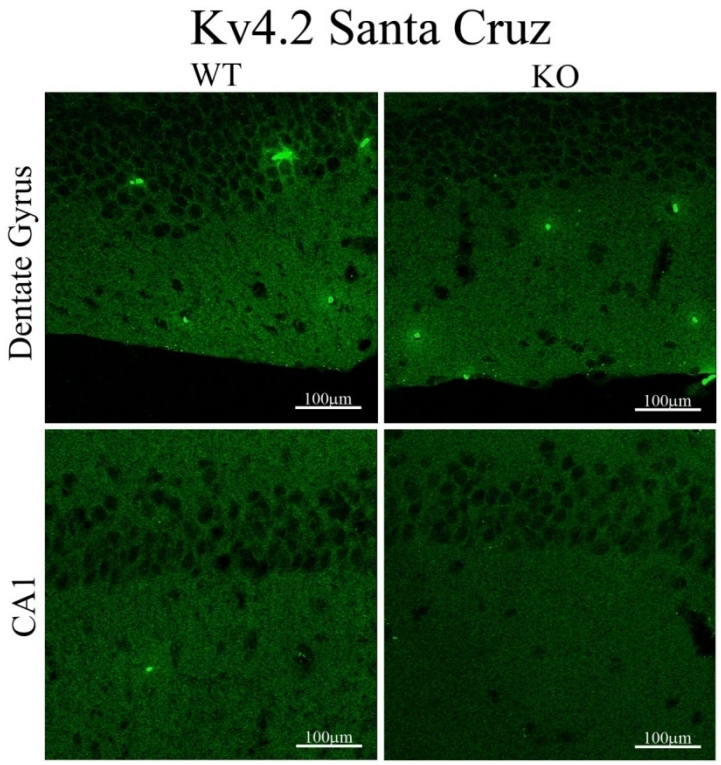

Figure 16. Kv4.2 protein is reduced in dendritic regions of the *Fmr1*-KO hippocampus. This is a representative immunostaining of quantitative analysis shown in Figure 17. I conducted fluorescence immunostainings using a specific, anti-goat Kv4.2 antibody from Santa Cruz on hippocampal brain sections of wild type and *Fmr1* knockout (KO) in the dentate gyrus and CA1 regions.

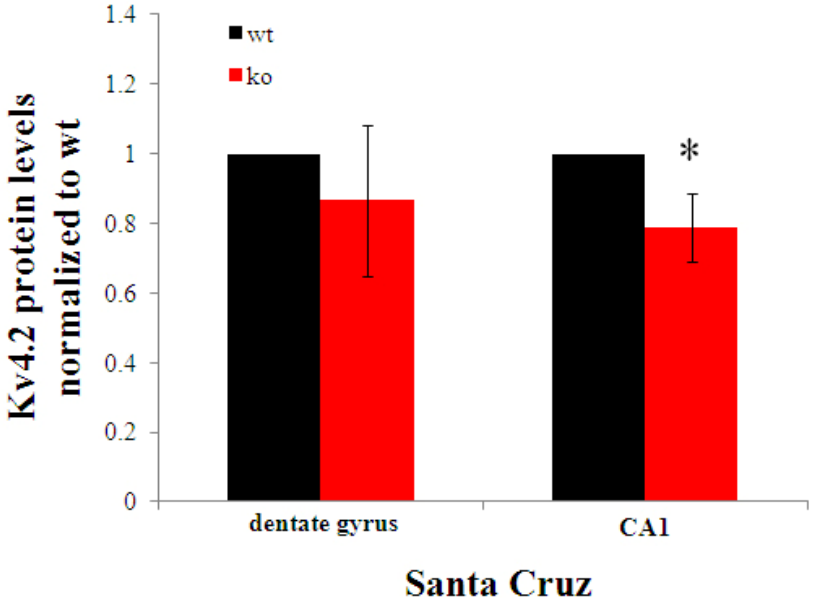

Figure 17. Kv4.2 protein is reduced in hippocampal dendrites of the *Fmr1* knockout mouse. Quantification of Kv4.2 protein in the dendrites of the dentate gyrus (DG) and CA1 region of the hippocampus showed significant downregulation of Kv4.2 protein in the *Fmr1* knockout (KO). KO signal intensities were normalized to the wild type (WT) in each experiment. Quantitative analysis of Kv4.2 immunostainings showed a 13% reduction trend of Kv4.2 protein in the KO DG (n=5, paired t-test, p= 0.235). Quantitative analysis of Kv4.2 immunostainings in the CA1 region showed a significant 21% reduction (n=5, paired t-test, *p= 0.01).

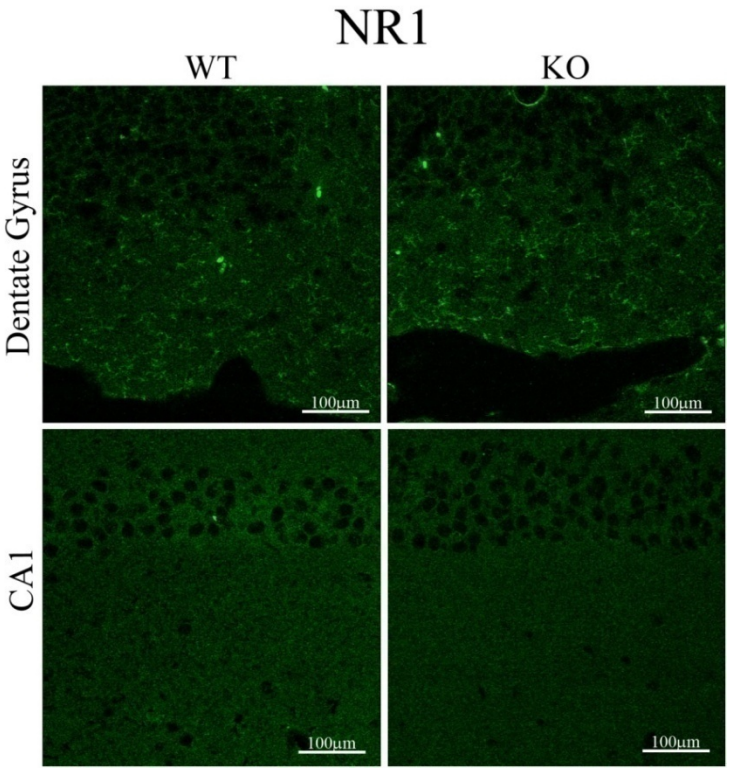

Figure 18. NR1 shows no change in the *FMR1*-KO in hippocampal dendrites. This is a representative immunostaining of quantitative analysis shown in Figure 19. I conducted fluorescence immunostainings using a specific, anti-rabbit NR1 antibody from Chemicon on hippocampal brain sections of wild type and *FMR1* knockout (KO) in the dentate gyrus and CA1 regions.

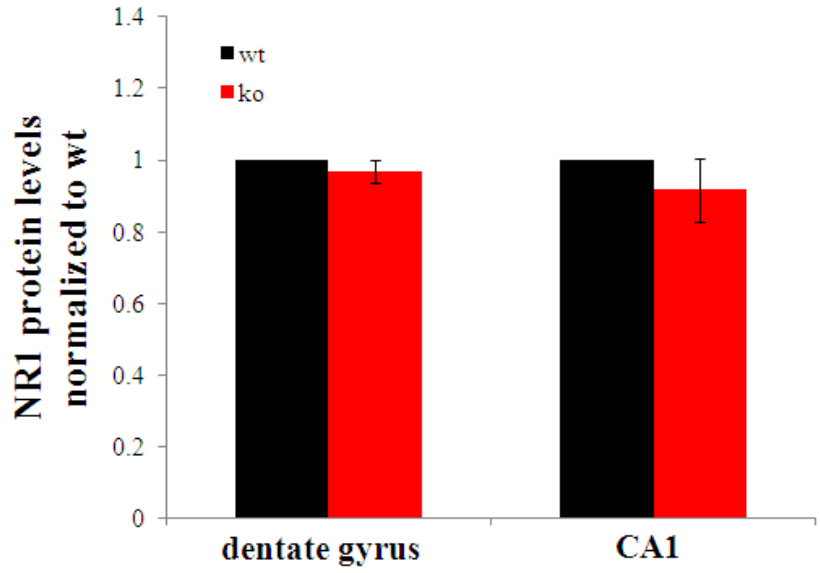

Figure 19. NR1 protein shows no significant change in the *Fmr1* knockout hippocampus. Quantification of NR1 protein in the dendrites of the dentate gyrus (DG) and CA1 region of the hippocampus showed no significant change of protein expression in the *Fmr1* knockout. KO signal intensities were normalized to WT in each experiment. Quantitative analysis of NR1 immunostainings showed a 3% reduction trend in the KO DG (n=3, paired t-test, p=0.21) which is not significant. Similarly, quantitative analysis of NR1 immunostainings showed a 8% reduction trend in the KO CA1 region (n=3, paired t-test, p=0.25) which is not significant.

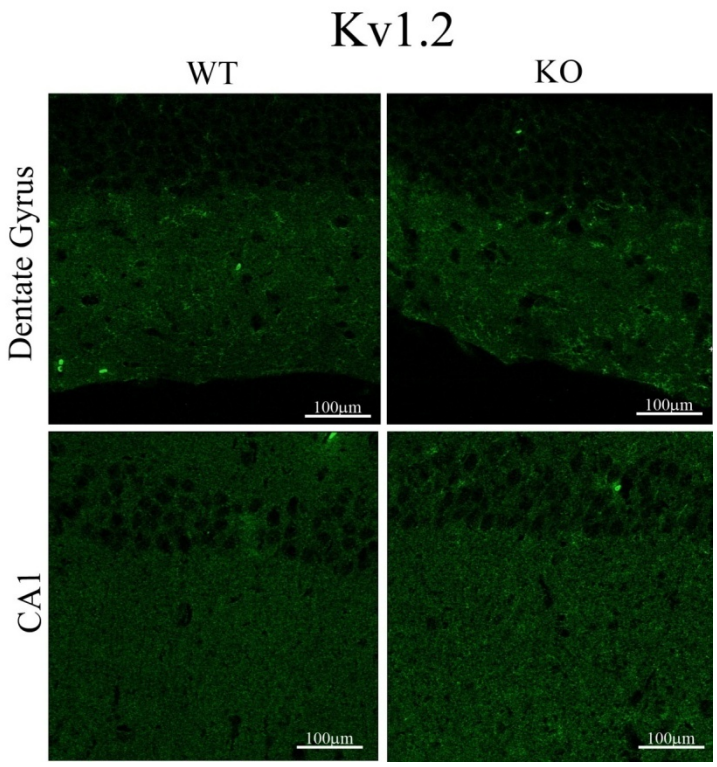

Figure 20. Kv1.2 shows change in the *Fmr1*-KO in hippocampal dendrites. This is a representative immunostaining of quantitative analysis shown in Figure 21. I conducted fluorescence immunostainings using a specific, anti-mouse Kv1.2 antibody from Neuromab on hippocampal brain sections of wild type and *Fmr1* knockout (KO) in the dentate gyrus and CA1 regions.

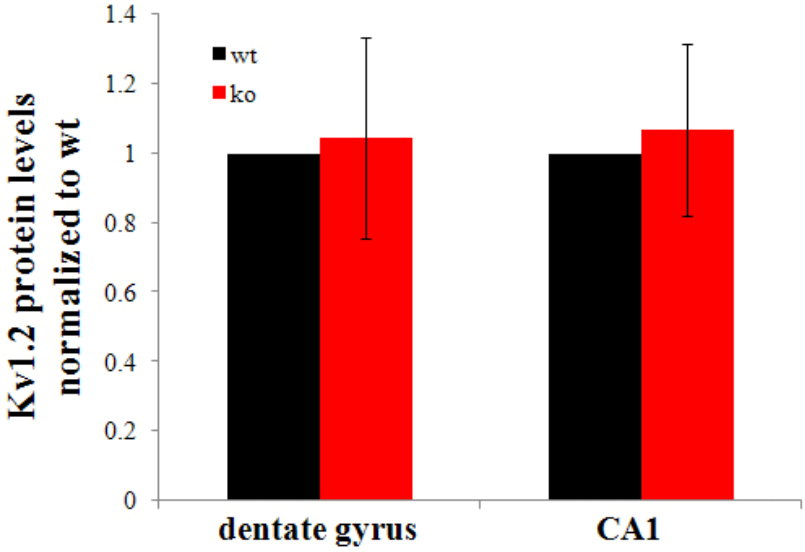

Figure 21. Kv1.2 protein shows no significant change in the *Fmr1* knockout hippocampus. Quantification of Kv1.2 protein in the dendrites of the dentate gyrus (DG) and CA1 region of the hippocampus showed no significant change of protein expression in the *Fmr1* knockout. KO signal intensities were normalized to WT in each experiment. Quantitative analysis of Kv1.2 immunostainings showed a 4% upregulation trend in the KO DG (n=4, paired t-test, p=0.750) which is not significant. Similarly, quantitative analysis of Kv1.2 immunostainings showed a 7% upregulation trend in the KO CA1 region (n=4, paired t-test, p=0.571) which is not significant.

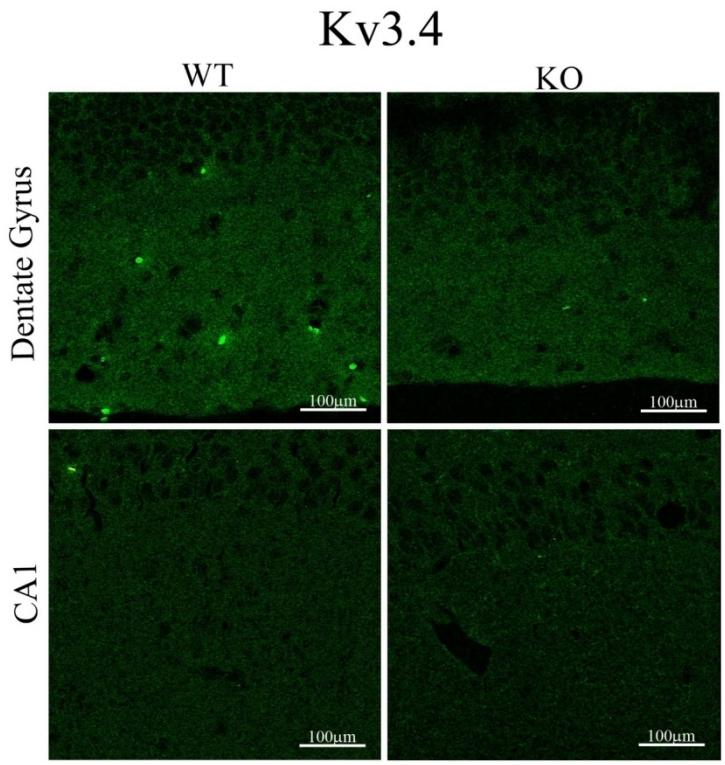

Figure 22. Kv3.4 shows no change in the *Fmr1*-KO in hippocampal dendrites. This is a representative immunostaining of quantitative analysis shown in Figure 23. I conducted fluorescence immunostainings using a specific, anti-mouse Kv3.4 antibody from Neuromab on hippocampal brain sections of wild type and *Fmr1* knockout (KO) in the dentate gyrus and CA1 regions.

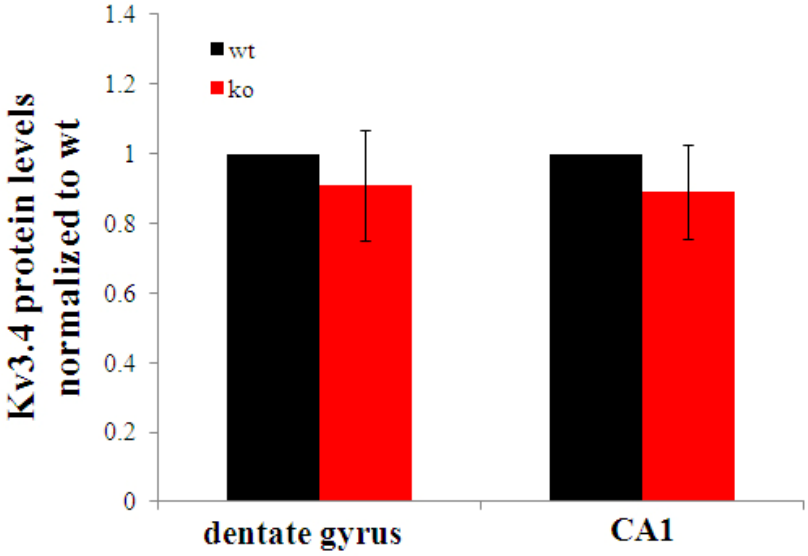

Figure 23. Kv3.4 protein shows no significant change in the *Fmr1* knockout hippocampus. Quantification of Kv3.4 protein in the dendrites of the dentate gyrus (DG) and CA1 region of the hippocampus showed no significant change of protein expression in the *Fmr1* knockout. KO signal intensities were normalized to the WT in each experiment. Quantitative analysis of Kv3.4 immunostainings showed a 9% reduction trend in the KO dentate gyrus (n=4, paired t-test, p=0.27) which is not significant. Similarly, quantitative analysis of Kv3.4 immunostainings showed an 11% reduction trend in the KO CA1 region (n=4, paired t-test, p=0.14) which is not significant.

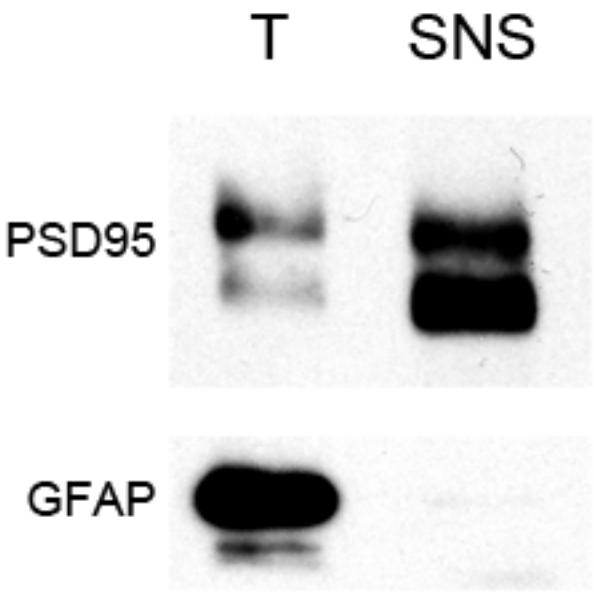

Figure 24. Western Blot analyses with antibodies specific for PSD95 (top) and GFAP (bottom) demonstrate purity of synaptoneurosomal preparations. The postsynaptic protein PSD95 is enriched in SNS compared to total homogenate (T), whereas virtually no Glial fibrillary acidic protein (GFAP) can be detected. This indicated that SNS fractions are enriched in synaptic compartments, and practically free of glia cell contamination.

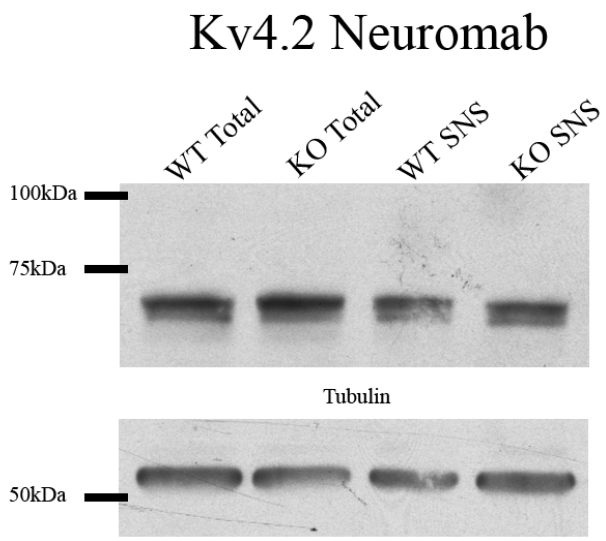

Figure 25. Kv4.2 shows no change in brain lysates and synaptoneurosomes from *Fmr1* KO mice compared to WT. This is a representative western blot of quantitative analysis shown in Figure 26. I conducted western blot analyses using a specific, anti-mouse Kv4.2 antibody from Neuromab on total and synaptoneurosome (SNS) preparations of wild type (WT) and *Fmr1* knockout (KO) brains.

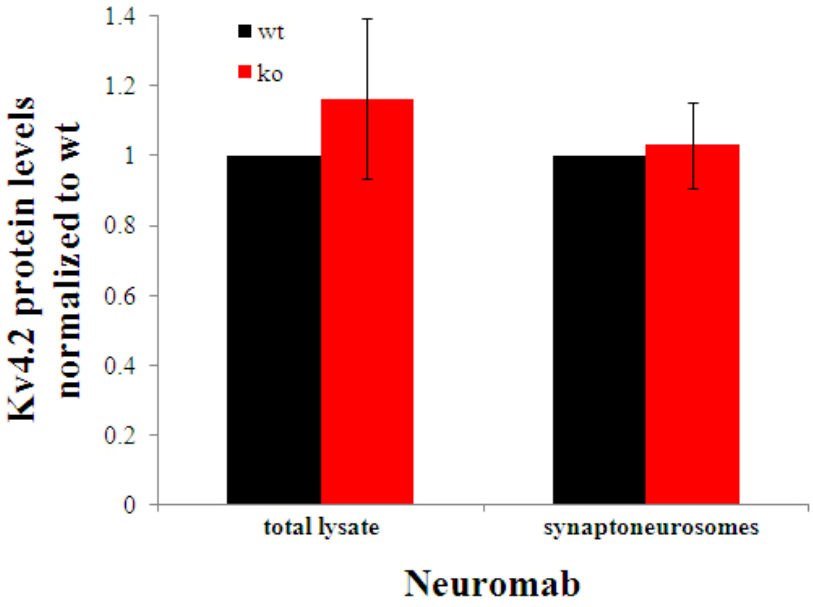

Figure 26. Kv4.2 shows no significant change in *Fmr1* KO protein extracts. Western blot analyses using a specific, anti-mouse Kv4.2 antibody from Neuromab on total and synaptoneurosome (SNS) preparations of wild type (WT) and *Fmr1* knockout (KO) mouse brains showed an upregulation trend in knockout. Quantification of the Kv4.2 protein showed a 16% upregulation trend (n=4, paired t-test, p=0.249) in the total lysate which is not statistically significant. Similarly, the synaptoneurosome preparation of the KO showed a 3% upregulation trend (n=4, paired t-test, p=0.661) that is also not statistically significant. Kv4.2 protein levels were normalized to α-tubulin.

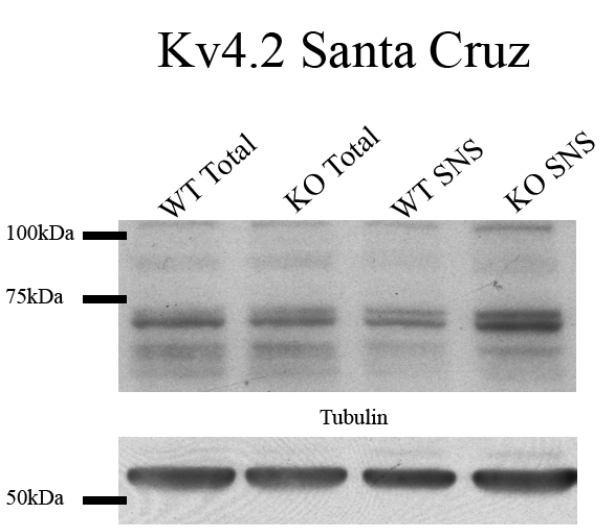

Figure 27. Kv4.2 shows no change in brain lysates and synaptoneurosomes from *Fmr1* KO mice compared to WT. This is a representative western blot of quantitative analysis shown in Figure 28. I conducted western blot analyses using a specific, anti-goat Kv4.2 antibody from Santa Cruz on total and synaptoneurosome (SNS) preparations of the wild type (WT) and *Fmr1* knockout (KO) brains.

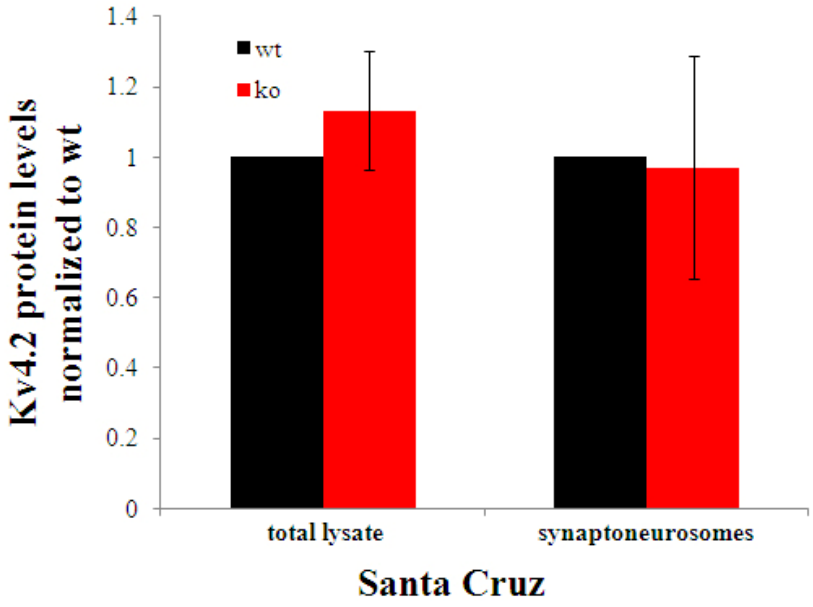

Figure 28. Kv4.2 shows no significant change in the *Fmr1* KO protein extracts. Western blot analyses using a specific, anti-goat Kv4.2 antibody from Santa Cruz on total and synaptoneurosome (SNS) preparations of the wild type (WT) and *Fmr1* knockout (KO) mouse brains showed an upregulation trend in knockout. Quantification of the Kv4.2 protein showed a 13% upregulation trend (n=3, paired t-test, p=0.307) in the total lysate which is not statistically significant. The synaptoneurosome preparation of the KO showed a 3% downregulation trend (n=3, paired t-test, p=0.887) that is also not statistically significant. Kv4.2 protein levels were normalized to α-tubulin.

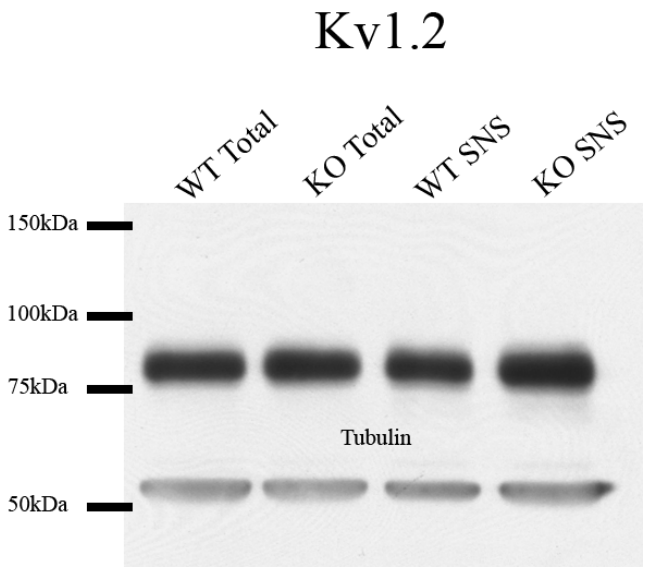

Figure 29. Kv1.2 shows no change in brain lysates and synaptoneurosomes from *Fmr1* KO mice compared to WT. This is a representative western blot of quantitative analysis shown in Figure 30. I conducted western blot analyses using a specific, anti-mouse Kv1.2 antibody from Neuromab on total and synaptoneurosome (SNS) preparations of the wild type (WT) and *Fmr1* knockout (KO) brains.

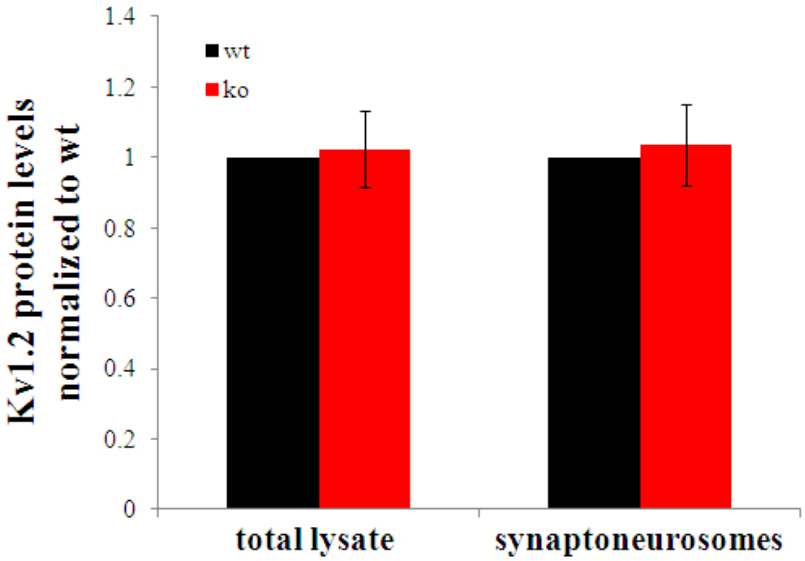

Figure 30. Kv1.2 shows no significant change in *Fmr1* KO protein extracts. Western blot analyses using a specific, anti-mouse Kv1.2 antibody from Neuromab on total and synaptoneurosome (SNS) preparations of the wild type (WT) and *Fmr1* knockout (KO) mouse brains showed an upregulation trend in knockout. Quantification of the Kv1.2 protein showed a 2% upregulation trend (n=5, paired t-test, p=0.649) in the total lysate which is not statistically significant. Similarly, the synaptoneurosome preparation of the KO showed a 4% upregulation trend (n=5, paired t-test, p=0.533) that is also not statistically significant. Kv1.2 protein levels were normalized to α-tubulin.

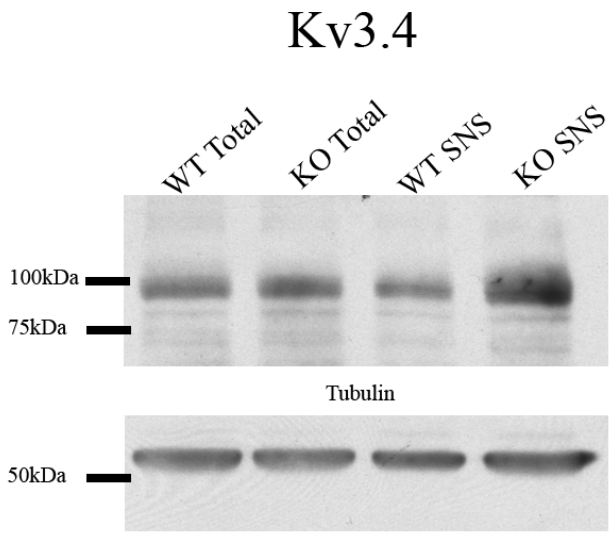

Figure 31. Kv3.4 shows no change in brain lysates and synaptoneurosomes from *Fmr1* KO mice compared to WT. This is a representative western blot of quantitative analysis shown in Figure 32. I conducted western blot analyses using a specific, anti-mouse Kv3.4 antibody from Neuromab on total and synaptoneurosome (SNS) preparations of the wild type (WT) and *Fmr1* knockout (KO) brains.

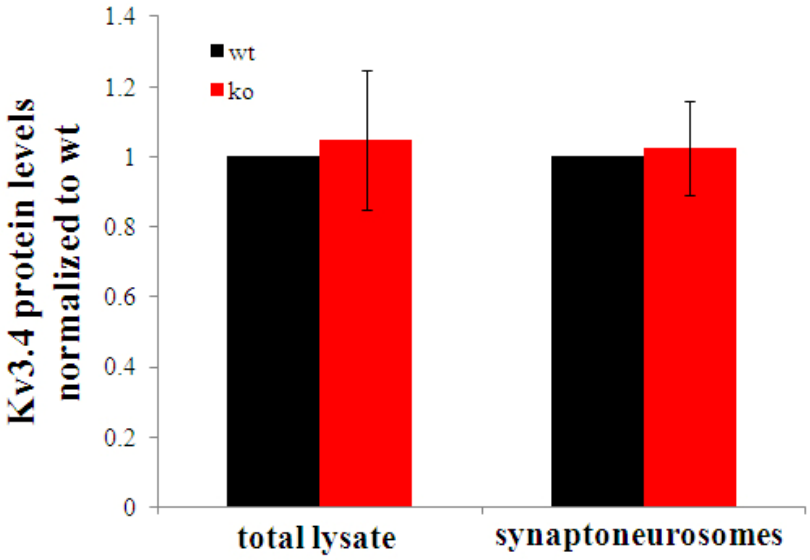

Figure 32. Kv3.4 shows no significant change in the *Fmr1*-KO in hippocampal dendrites. Western blot analyses using a specific, anti-mouse Kv3.4 antibody from Neuromab on total and synaptoneurosome (SNS) preparations of the wild type (WT) and *Fmr1* knockout (KO) mouse brains showed an upregulation trend in knockout. Quantification of the Kv3.4 protein showed a 5% upregulation trend (n=5, paired t-test, p=0.621) in the total lysate which is not statistically significant. Similarly, the synaptoneurosome preparation of the KO showed a 2% upregulation trend (n=5, paired t-test, p=0.741) that is also not statistically significant. Kv3.4 protein levels were normalized to α-tubulin.

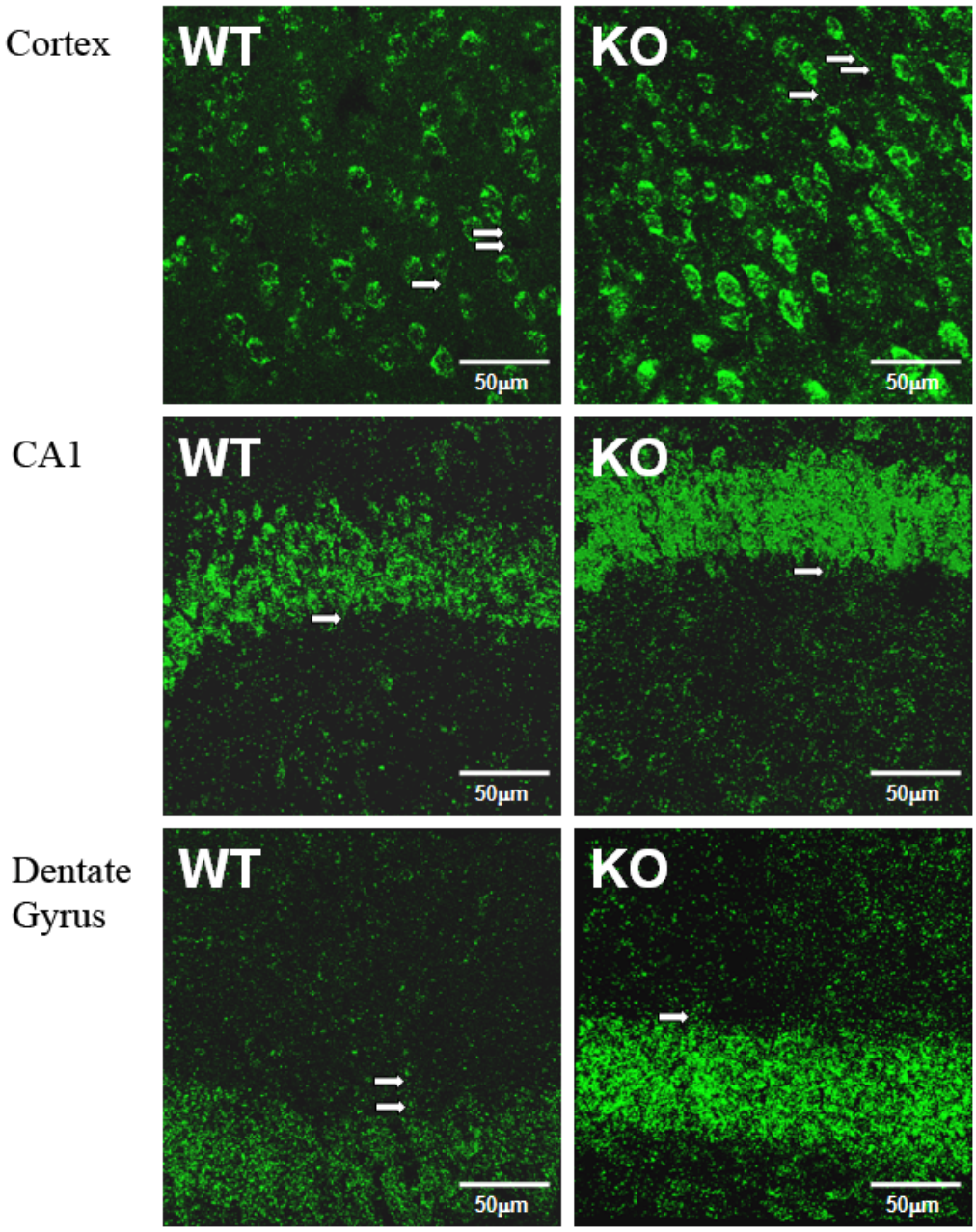

Figure 33. Kv4.2 mRNA may localize in dendrites of the mouse cortex as well as the CA1 and dentate gyrus regions of hippocampus. Kv4.2 mRNA (green) is localized to the dendritic layers of the mouse cortex and areas of the hippocampus linked to human temporal lobe epilepsy. Arrows highlight individual dendrites with Kv4.2 mRNA. High background staining made it difficult to absolutely report that Kv4.2 mRNA localized in these regions. In the lower four boxes, strong green signal is shown in the cell body layer of the dentate gyrus and CA1. Kv4.2 mRNA dendritic localization occurs in both the wild type (WT) and *Fmr1* knockout (KO). Dentritic localization of Kv4.2 mRNA suggests that Kv4.2 may be locally translated in dendrites.

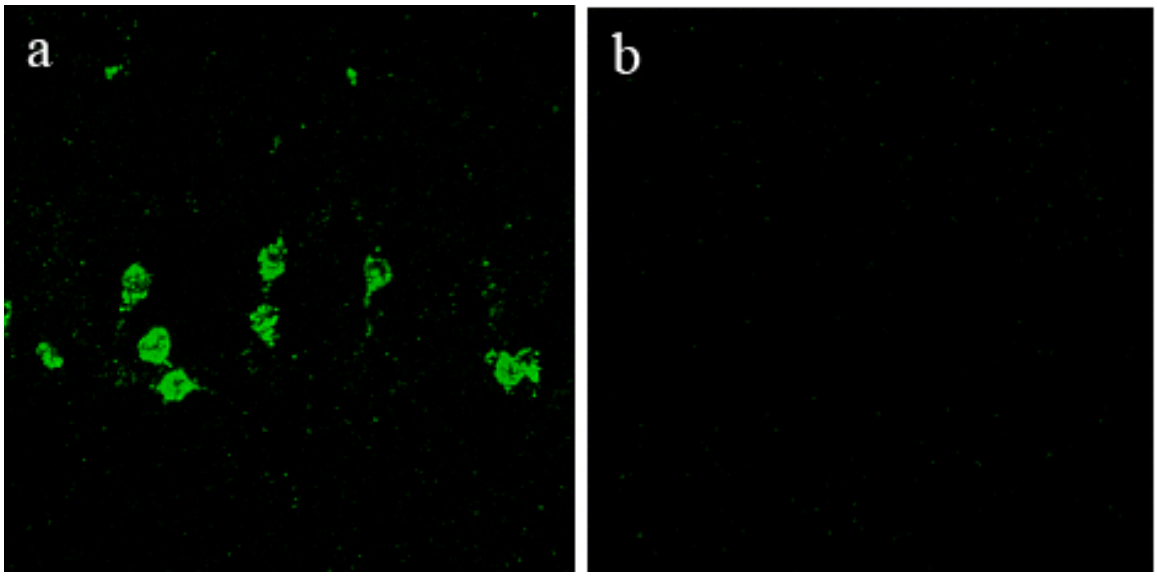

Figure 34. Arg3.1 mRNA serves as a positive control for in situ hybridizations. (A) Arc/Arg3.1-specific fluorescent *in situ* hybridization (FISH) demonstrates the characteristic pattern of Arc/Arg3/1 mRNA in the dentate gyrus with single highlighted cells. (B) In contrast, FISH with a sense Arc/Arg3.1 riboprobe showed no signal above background staining. This is a proof of principle that the applied FISH protocol is suitable to specifically detect mRNAs in the hippocampus.